BIODIVERSITAS
Volume 26, Number 8, August 2025
Pages: 3994-4016

ISSN: 1412-033X
E-ISSN: 2085-4722
DOI: 10.13057/biodiv/d260829

Polystyrene biodegradation and functional biodiversity of gut microbial consortia in *Tenebrio molitor* with metagenomic and metabolomic insights

AFANDI, SONY SUHANDONO, POPI SEPTIANI, AZZANIA FIBRIANI♥
School of Life Sciences and Technology, Institut Teknologi Bandung. Jl. Ganeca No. 10, Bandung 40132, West Java, Indonesia. Tel.: +62-22-2511575, Fax.: +62-22-2534107, ♥email: afibriani@itb.ac.id

Manuscript received: 10 April 2025. Revision accepted: 19 August 2025.

Abstract. *Afandi, Suhandono S, Septiani P, Fibriani A. 2025. Polystyrene biodegradation and functional biodiversity of gut microbial consortia in* Tenebrio molitor *with metagenomic and metabolomic insights. Biodiversitas 26: 3994-4016.* Polystyrene (PS), a persistent plastic pollutant, can be biodegraded by *Tenebrio molitor* larvae through gut microbiome-mediated processes. This study employed integrated shotgun metagenomics and metabolomics to elucidate the microbial taxa, enzymes, and metabolic pathways involved in PS degradation. In vivo trials demonstrated a PS mass reduction of 6.38%, while in vitro experiments using gut microbial consortia resulted in a 3.49% mass loss. Surface erosion of the PS film was confirmed via scanning electron microscopy. Taxonomic profiling identified 334 bacterial genera under the PS diet and 329 under rice bran, with 93 genera unique to PS treatment. Dominant phyla included Proteobacteria (53.87%), Actinobacteria (6.44%), and Aquificae (6.42%). Hydrocarbon-degrading genera enriched under the PS diet included Burkholderia (3.94%), Nocardioides (2.67%), and Oceanobacter, the latter being exclusive to PS-fed larvae. Biodiversity metrics revealed high genus-level diversity (Shannon Index H′ = 3.79-3.81), moderate Evenness (E = 0.65-0.66), and low Dominance (D = 0.06), indicating a complex yet balanced microbial ecosystem under xenobiotic stress. Functional annotations identified xenobiotic degradation pathways, including styrene metabolism (0.56%) and toluene metabolism (1.40%), driven by key enzymes such as monooxygenases and phenylacetaldehyde dehydrogenase. Metabolomic profiling identified 39 metabolites in larval frass and 20 degradation intermediates in the liquid medium, with lactic acid and benzyl alcohol being the primary products associated with the breakdown of aromatic compounds. These findings underscore the functional biodiversity and ecological adaptability of the gut microbiome in plastic detoxification, highlighting insect-microbe symbioses as promising agents for sustainable bioremediation strategies.

Keywords: Insect gut microbiome, plastic degradation, shotgun metagenomics, *Tenebrio molitor*, xenobiotic metabolism

INTRODUCTION

Polystyrene (PS) pollution has become a pressing global challenge due to its extensive use in disposable products and its resistance to natural degradation. Despite advances in chemical and biological degradation, the inherent stability of PS's carbon–carbon backbone limits efficiency and scalability (Ho et al. 2018; Quan et al. 2023). Recent findings that certain insect larvae can ingest and process synthetic polymers have opened new perspectives for eco-friendly bioremediation. Among these insects, *Tenebrio molitor* (Linnaeus, 1758) larvae (mealworms) have been highlighted as a promising biological model in plastic waste management, combining ecological adaptability with practical applicability (Wang et al. 2022). Remarkably, mealworms can degrade PS foam within 24 hours (Yang et al. 2015), a process largely mediated by their gut microbiome rather than by the insect alone.

The gut microbiome forms a symbiotic system that catalyzes the breakdown of complex polymers into assimilable metabolites. Such mutualistic interactions are widespread in insects: termites digest lignocellulose with microbial aid, while aphids rely on endosymbionts for nitrogen metabolism. These examples reflect evolutionary strategies of co-adaptation, where host and microbes expand ecological niches under dietary or environmental pressures. The insect gut microbiome is thus increasingly recognized as a reservoir of genetic and enzymatic potential for biotechnology (Urbanek et al. 2020; Muñoz-Benavent et al. 2021).

Insect guts harbor diverse microbial ecosystems—including bacteria, archaea, fungi, and protozoa—shaped by host phylogeny, gut morphology, developmental stage, diet, and habitat (Yun et al. 2014; López-Hernández et al. 2025). For termites and ants, gut symbionts are vertically transmitted, reflecting long co-evolutionary histories (Sanders et al. 2014; Mikaelyan et al. 2015). By contrast, beetles such as *T. molitor* acquire more environmentally determined microbial assemblages, yet retain core metabolic traits. This pattern suggests ecological filtering and functional convergence within insect-microbe systems.

Functionally, these microbes facilitate nutrient acquisition, detoxification, and immune regulation, extending their impact to biogeochemical cycles, organic matter turnover, and pollutant transformation (Mondal et al. 2023). In PS degradation, microbial enzymes—including monooxygenases, cytochrome P450s, peroxidases, and dehydrogenases—work synergistically to depolymerize PS into less persistent metabolites (Lou et al. 2020; Venegas et al. 2024). Host physiology further enhances these processes through

mechanical breakdown in the gut and secretion of emulsifying compounds, demonstrating a complex interplay between insect and microbiota.

Other insects, including *Galleria mellonella* (wax moth larvae) and *Zophobas atratus* (superworms), have also shown the capacity to degrade plastics (Kundungal et al. 2021; Bai et al. 2023; He et al. 2024). These findings suggest that plastic biodegradation is not restricted to a single species but may be an emergent ecological trait across multiple insect lineages. However, most gut microbial diversity remains uncultured under laboratory conditions, limiting the identification of key degradative taxa and pathways (Bai et al. 2023; He et al. 2024).

To address these constraints, culture-independent tools such as metagenomics and metabolomics have become essential. Shotgun metagenomics enables community-wide genetic profiling and the detection of functional genes related to plastic degradation (Quince et al. 2017). For example, Lepcha et al. (2025) used metagenomics to reveal over nine million ORFs from landfill microbiomes, offering new insights into microbial functions under extreme conditions. Similarly, Wright et al. (2021) showed active biodegradation of PET in marine environments by linking gene abundance to evidence of polymer oxidation. Metabolomics complements these approaches by identifying intermediate metabolites and host–microbe responses during degradation (Mishra et al. 2021; Chang et al. 2024). Together, these approaches provide a systems-level view of biodegradation mechanisms in insect guts.

Despite growing attention, few studies have combined metagenomic and metabolomic analyses to fully unravel PS degradation in *T. molitor*. Prior findings show shifts in gut microbial structure and enzyme activity under PS exposure (Wu et al. 2022), yet links to metabolic output and degradation efficiency remain poorly defined. Integrated multi-omics approaches can bridge this gap by mapping networks that connect microbial taxa, functional enzymes, and metabolic pathways (Chang et al. 2024).

Understanding PS degradation through insect-microbe symbiosis not only addresses a critical pollution issue but also deepens our appreciation of microbial biodiversity and evolutionary innovation. Therefore, this study aimed to investigate the microbial and metabolic pathways underlying PS degradation in *T. molitor* larvae using an integrated shotgun metagenomics and metabolomics approach.

MATERIALS AND METHODS

Preparation of mealworm and mealworm gut suspension

Mealworms were obtained from commercially available animal feed suppliers in Bandung and identified as *Tenebrio molitor* based on the beetle identification guide (Robinson 2005; Calmont and Soldati 2008). *T. molitor* larvae used in the experiment were at the 11th-instar stage with a body length of 11-12 mm and a weight of 60-80 mg. All mealworms were fed Rice Bran (RB) and starved for 48 hours before switching to the experimental diet.

Preparation of suspension samples

Ten samples of mealworms were sterilized with 70% alcohol. The mealworms were then dissected with sterile scissors, and their guts were extracted with a scalpel. The guts were transferred to a centrifuge tube containing 200 µL of sterile physiological solution and homogenized with a mini-grinder pestle to obtain a mealworm gut suspension.

Plastics

PS materials used were PS foam, PS pellets, and PS film. PS foam was sourced from Styrofoam packaging waste. It was cut into 2 cm^3 cubes, weighed to obtain 1 g, and utilized as feed for mealworms. PS film (Good Fellow GF93064585, Merck-Millipore) was prepared for experimentation. The PS films were aseptically transferred into a 70% (vol/vol) ethanol solution and left for 30 minutes. Each film was then placed into a sterile Petri dish, incubated at 45-50°C overnight for drying, and subsequently equilibrated to room temperature. The sterilized films were then introduced into a liquid medium and incubated with mealworm gut extract. Additional samples were prepared for Scanning Electron Microscopy (SEM) analysis.

PS pellets (Sigma Aldrich 331651-500G, Merck-Millipore) were used to prepare PS emulsions and powder. Subsequently, the mealworm gut microbiome consortium utilized these emulsions for the in vitro analysis of PS biodegradation. PS powder for gravimetric biodegradation analysis was obtained by grinding PS pellets with a mortar, sieving the resulting through a 50-mesh sieve. The PS powder was weighed and transferred into pre-weighed sterile glass Petri dishes. The samples were then irradiated using a long-wave UV lamp (365 nm) for 7 days. During irradiation, the Petri dishes with the powder were positioned 50 cm away from the lamp.

Polystyrene sterility measures

Following UV irradiation, the sterility of the PS powder was confirmed by aseptic transfer of samples into sterile Tryptic Soy Broth TSB and Fluid Thioglycollate Medium. These cultures were incubated for 14 days at 30°C, with daily monitoring for turbidity. Only PS powder samples exhibiting no microbial growth after this period were considered sterile for subsequent biodegradation experiments.

Preparation of polymer emulsion plastic

Two grams of PS pellets were dissolved in 40-60 mL of dichloromethane (Merck). The solution was then mixed with 2 mL of 2% Sarkosyl (Sigma Aldrich) and 100 mL of distilled water. To remove the dichloromethane, the mixture was sonicated for 10 minutes and then stirred in a draft chamber at 80°C for two hours. The polymer emulsion was completed by adding 400 mL of distilled water. The pH of the solution was adjusted to 7.0 using KOH (Merck) (Urbanek et al. 2020).

Metagenomic analysis of mealworm gut under PS diet treatment

Mealworm rearing

The experiment consisted of three replicate treatment groups, each containing 50 mealworms. Across all

experimental treatments, mealworms were maintained in 1.5-L polypropylene containers and incubated in darkness for 24 hours at 24.13±0.01°C with a relative humidity of 57.48±0.09%, over 28 days 28 days. Mealwporms' survival rate, weight, and PS consumption were monitored every four days. Frass from each treatment was collected and stored at -20°C for further analysis. The experiment was conducted in triplicate with the following treatment: RB1 (mealworms were fed 1 g of rice bran (control)) mealworms were fed 1 g of rice bran (control)), PS1 (mealworms were fed 1 g of PS foam), (mealworms were fed 1 g of PS foam), and PS+RB (mealworms were fed 1 g of rice bran and 1 g of PS). PS foam degradation was evaluated based on the percentage of weight loss using the following formula (Kundungal et al. 2019):

$$Weight\ loss\ (\%) = \left(\frac{\text{Initial weight} - \text{Final weight}}{\text{Initial weight}}\right) x\ 100$$

In vitro biodegradation of PS film

Two experimental conditions were tested: (i) PS film in BH medium without mealworm gut extract (control), and (ii) PS film with 1 mL of mealworm gut extract (samples). All PS films were incubated in 100 mL of BH medium at 30°C in a shaker incubator with an agitation speed of 120 rpm for 28 days. Morphological alterations in the PS films due to mealworm gut microbial activity were investigated using specific pre-SEM treatments. Microbial colonization on the PS film surface was examined after the films were washed with distilled water. Surface damage was assessed by immersing both control and treated PS films in a 2% (wt/vol) SDS solution for 4 hours (Zhang et al. 2024), followed by rinsing the films three times with distilled water to remove SDS and any residual microorganisms.

In vitro biodegradation of PS powder

To evaluate the biodegradation potential of mealworm gut microbiota, a biodegradation assay was conducted using three replicated Erlenmeyer flasks containing Bushnell-Haas (BH) liquid medium supplemented with PS powder. The PS powder was added to reach a final concentration of 1% (v/v). Each flask was inoculated with 1 mL of mealworm gut extract and incubated at 30°C with continuous agitation at 120 rpm for 28 days. During the incubation period, the total weight of the medium, including PS particles, was measured at four-day intervals (on days 0, 4, 8, 12, 16, 20, 24, and 28). The extent of plastic degradation was quantified by calculating the percentage of PS weight loss over time, reflecting microbial activity and degradation efficiency under xenobiotic exposure.

Total Plate Count (TPC) analysis for bacterial quantification in the mealworm gut and BH medium

In this study, the Total Plate Count (TPC) method was employed to quantify bacterial populations in mealworm gut samples subjected to RB1, PS+RB1, and PS1 diet treatments on day 0 and day 28. For each treatment group and time point, composite gut suspensions were prepared by pooling gut extracts from ten individual larvae. A volume of 200 µL from each composite suspension was diluted with 800 µL of sterile physiological solution to obtain a final volume of 1 mL. Serial dilutions were then performed, and 100 µL aliquots from each dilution tube were inoculated into 20 mL of nutrient medium (Oxoid). Cultures were incubated at 30°C for 24 hours. Each dilution series was analyzed using duplicate composite samples, and bacterial colony counts were determined based on visible colony formation on the medium. The TPC method was also applied to assess the bacterial population in the Bushnell-Haas (BH) liquid medium during the in vitro biodegradation of PS powder. Samples were collected on day 0 and day 28, and a 1 mL aliquot from each was analyzed. Serial dilution was conducted, with 100 µL from each dilution tube transferred into 20 mL of nutrient medium (Oxoid) and incubated at 30°C for 24 hours. All dilutions were conducted in duplicate, and bacterial counts were calculated based on colony growth observed in the medium.

Metagenomic analysis of mealworm gut under PS diet treatment

DNA extraction

Metagenomic DNA was extracted from a composite sample derived from gut suspensions of ten *T. molitor* individuals collected on day 28 of the experimental period. The pooled sample was homogenized and subjected to DNA isolation using the DNeasy PowerSoil Pro Kit (Qiagen), strictly following the manufacturer's instructions. DNA integrity was verified using 1.0% agarose gel electrophoresis, and purity was assessed with a NanoDrop spectrophotometer (Thermo Fisher Scientific™). Samples were selected based on an A260/A280 ratio between 1.8 and 2.0, and a concentration greater than 30 ng/µL.

Library preparation and sequencing

The extracted metagenomic DNA was sent to Singapore Novogen for shotgun sequencing; the Illumina NovaSeq 6000 sequencing platform was utilized for sequencing. Shotgun metagenomic sequencing was performed on a single replicate of a composite metagenomic DNA sample. To construct the library, the genomic DNA was randomly fragmented into shorter pieces, followed by end repair, adapter ligation, and size selection (350-400 bp) using the Illumina TruSeq DNA PCR-Free Library Prep Kit to minimize amplification bias. Library validation is performed using Bioanalyzer and qPCR to ensure accurate quantification. Sequencing generating 150 bp paired-end reads with a target depth of ~6 Gb per sample, yielding an estimated sequencing depth of >40 million raw reads. Raw data quality was assessed using FastQC, and adapter trimming and quality filtering were performed using Trimmomatic to downstream bioinformatic analysis.

Raw reads quality control

The quality control of DNA sequences was performed using FastQC (version 0.11.9) with the graphical user interface (Andrews 2010) and visualized using MultiQC to summarize multiple reports in a single plot. This confirmed high sequencing quality (Q-score >30 across all bases) and the absence of adapter contamination. All raw reads (150 bp, paired-end; Illumina NovaSeq 6000) met quality

thresholds (Phred ≥20 in ≥95% of bases) and were therefore retained without trimming.

Metagenome assembly

The processing analysis was started by de novo de novo assembly using MEGAHIT version 1.2.9 (Li et al. 2015) with parameters set to --k-min 21, --k-max 141, --k-step 20, and --min-contig-length 200, resulting in contigs with an N50 of 2,143 bp and average coverage depth of approximately 45×. The output of the metagenome assembly, referred to as final contigs, was saved in a FASTA file for downstream analysis.

Protein alignment and database configuration

The assembled metagenomic contigs were aligned using DIAMOND version 0.9.24.125 (Buchfink et al. 2014) against the NCBI-nr database, which includes RefSeq, UniProtKB/Swiss-Prot, PDB, and PRF non-redundant coding sequences. The database was downloaded using the command wget ftp://ftp.ncbi.nlm.nih.gov/blast/db/FASTA/nr.gz and configured using diamond makedb --in nr.gz -d nr --masking 0. Alignment was performed using the diamond blastx command, which is significantly faster, up to 20,000 times faster up to 20,000 times faster than traditional BLASTX tools. DIAMOND processed only alignments with an expected (E) value threshold of 0.001, as described by Buchfink et al. (2014); the resulting Diamond Archive Alignment (DAA) file.

Taxonomic and functional profiling

Taxonomic and functional profiling was performed using MEGAN7 Ultimate Edition (MEGAN7 UE) (Huson et al. 2016), where DIAMOND output files in DAA format were indexed with the Meganizer tool and mapped against the Megan-map-Oct2019-ue.db reference database. This curated mapping file, obtained from the official MEGAN7 site, integrates multiple annotation sources, including NCBI Taxonomy for hierarchical classification, KEGG (Kyoto Encyclopedia of Genes and Genomes) Pathways for metabolic and enzymatic functions, COG for orthologous group assignment, InterPro2GO for protein domain and gene ontology predictions, and SEED Subsystems for subsystem-based functional annotation, enabling comprehensive insights into microbial diversity and ecological functionality.

Phylogenetic resolution via AnnoTree

To improve the accuracy of functional and taxonomic assignments, the AnnoTree database (Gautam et al. 2022) was employed. AnnoTree integrates GTDB-aligned taxonomy, offering high-resolution classification of uncultured and environmentally significant prokaryotic lineages. Importantly, this approach enabled systematic exclusion of host-derived genomes, specifically those affiliated with *T. molitor*, from metagenomic datasets.

Computational environment

All analyses were conducted on a high-performance Linux server equipped with 128 GB of RAM, 32 CPU cores, and 1 TB of SSD storage, ensuring efficient processing of large-scale metagenomic datasets.

Diversity, evenness, and dominance index calculations

Microbial diversity metrics were computed from taxonomic assignments obtained via MEGAN6. The Shannon Diversity Index (H') was calculated to assess community richness and evenness. In comparison, the Evenness Index (E) and Dominance Index (D) were used to describe distribution uniformity and the prevalence of dominant taxa, respectively. These indices were calculated following the equations described by Roswell et al. (2021) and classified according to Table 1.

To quantify taxonomic composition and assess community structure, sequencing reads were taxonomically assigned using MEGAN's binning algorithm, with classification resolved at the genus level. While shotgun metagenomics does not rely on traditional OTU clustering, taxonomic units identified at the lowest reliably assigned level per contig were used as a proxy for species-level diversity.

$$H' = \sum_{t=1}^{s} \frac{ni}{N} \ln \frac{ni}{N}$$

Where :
H' : Diversity Index
S : Number of species
ni : Individual number
N : Total individual number

$$E = \frac{H'}{\ln S}$$

Where :
E : Evenness Index
H' : Diversity Index
ln : Natural logarithm
S : No. of species

$$D = \sum \frac{ni}{N}$$

Where :
D : Dominance Index
ni : Individual number
N : Total individual number

Table 1. Diversity index value criteria

Index	Value	Criteria
Diversity	H′<1	Low
	1<H′<3	Moderate
	H′>1	High
Evenness	E<1	Low
	1<E<3	Moderate
	E>1	High
Dominance	D<1	Low
	1<D<3	Moderate
	D>1	High

Metabolomic analysis and in vitro PS degradation

Mealworm rearing

Metabolomic analysis was conducted by adapting the method developed by Tsochatzis et al. (2021a) with modifications. A total of 50 mealworms were reared in polypropylene boxes and fed exclusively with PS foam for seven days. Each treatment group was performed in triplicate under complete darkness at room temperature to maintain a controlled environment. On day seven, mealworms were dissected aseptically to extract their digestive tracts for in vitro PS degradation analysis. Gut samples were further processed for metabolomic analysis to identify the metabolite profile involved in PS degradation. All procedures were conducted under sterile conditions to minimize contamination and stress.

Preparation of extracts of PS degradation

PS emulsion was added to the Bushnell Haas (BH) liquid medium at a concentration of 1% (w/v), resulting in a final volume of 500 mL. On the first day, 50 mL of the medium was extracted using ethyl acetate. The remaining medium was subsequently mixed with 1 mL of mealworm gut cell extract and incubated at 30°C in a shaker incubator with an agitation speed of 120 rpm. Sampling was performed every four days (days 4, 8, 12, 16, 20, 24, and 28), with 50 mL of medium collected and extracted with ethyl acetate at each time point.

One gram of composite mealworm frass collected from days 0 to 28 (frass RB1, frass PS1, and frass PS+RB samples) and 50 mL of BH liquid medium collected on days 0, 4, 8, 12, 16, 20, 24, and 28 were mixed with 50 mL ethyl acetate; the mixture was gently shaken for 15 minutes to facilitate the extraction of organic compounds. After phase separation, the ethyl acetate layer was carefully collected for further analysis. Samples used in this analysis were non-replicated composite pools, intended for exploratory metabolite profiling and preliminary comparison of biodegradation-related chemical signatures.

Gas Chromatography-Mass Spectrometry (GC-MS) analysis

Liquid samples were subjected to derivatization to enhance chromatographic separation, improve peak shape, and optimize analyte response, particularly for fatty acids and volatile compounds. The crude extracts soluble in methanol were analyzed using GC-MS instrumentation (Agilent 7890B for GC and 5977A for MSD). The mass spectrometer (Agilent, 19091S-433: 93. DB-5MS UI, 5% Phenyl Methyl Silox) was directly coupled to a fused silica HP-5 capillary column (30 m × 0.25 mm i.d., 0.25 µm film thickness). The temperature program initiated at 40°C with a 1-minute hold, followed by a ramp of 10°C/min up to 325°C, and an isothermal hold for 20 minutes. The total runtime ranged from 30 to 40 minutes. Helium served as the carrier gas at a constant flow rate of 1.2 mL·min^{-1}. Approximately 1 µL of sample was injected into the system, with the injector maintained at 300°C. Mass spectra were processed using integrated software, and compounds were identified by matching fragmentation patterns against the National Institute of Standards and Technology (NIST 17/L) library. Compound annotation was further confirmed by comparing retention indices and ensuring consistency with chemical structures. Detected metabolites, including short-chain fatty acids, alcohols, esters, and hydrocarbons, were reported along with their relative abundance derived from peak area percentages (Srikandace et al. 2025).

Assessment of PS biodegradation

Frass analysis using Fourier Transform Infrared Spectroscopy (FTIR)

Fourier-transform infrared spectroscopy (FTIR) was employed to characterize functional groups in frass samples using a Thermo Scientific™ Nicolet™ iS™ 5 FTIR spectrometer. For each diet treatment group (RB1, PS1, PS+RB), a single replicate composite frass sample was prepared by pooling approximately 100 mg of larval feces collected periodically from days 4 to 28 of the experiment. In addition to frass samples, virgin Rice Bran (RB) and virgin Polystyrene (PS) foam were also analyzed as references. Spectral analysis was conducted in total reflection mode, covering a wavenumber range of 4000 to 400 cm^{-1}. This setup enabled comparative profiling of surface functional groups to assess chemical modifications resulting from gut-mediated interactions with xenobiotic substrates.

SEM analysis of PS film morphology

The morphology of PS films was examined using a Scanning Electron Microscope (SEM; JEOL JSM IT-300, Japan) to assess surface alterations after exposure. SEM analysis was conducted on a single replicate of PS film for each treatment. The samples included (i) PS film incubated without gut extract and washed with SDS, (ii) PS film incubated without SDS washing, and (iii) PS film subjected to SDS washing after incubation. All samples were collected on day 28. Before SEM imaging, each film was sputter-coated with a thin layer of gold (~10 nm) to enhance conductivity. Imaging was performed at an accelerating voltage of 20 kV, enabling high-resolution observation of surface morphology and potential degradation features across treatments.

Statistical analysis

Statistical analysis was performed using GraphPad Prism software (version 10.4.0) and Minitab Statistical Software (version 19.2020.1). Substantial differences in survival rate, weight change, TPC, and PS consumption were evaluated using a One-Way ANOVA (n = 3) with Tukey's and Tamhane's T2 post-hoc tests. Principal Component Analysis (PCA) for metabolite profiling was conducted using OriginPro 2024.

RESULTS AND DISCUSSION

Survival and growth of mealworms

After 28 days of dietary treatment, mealworms fed exclusively on the PS (PS1) diet exhibited the lowest Survival Rate (SR) at 89.99% (Figure 1.A). In contrast,

those fed with a combination of PS and rice bran (PS+RB) achieved a significantly higher SR of 99.67%. The higher mortality in the PS1 group can be attributed to the lack of adequate nutritional content in PS, which was essential for sustaining the growth and development of mealworms. The proximate analysis of rice bran indicates its nutrient-rich composition, consisting of 17.11% ash, 3.36% fat, 5.31% protein, and 69% carbohydrates. The proximate composition of rice bran used in this study was analyzed at the Balai Besar Industri Agro (BBIA), Bogor, Indonesia. These nutrients are crucial for maintaining the metabolic processes and energy requirements of mealworms. As a feed commonly sourced from agricultural and food processing industries, rice bran provides a balanced diet that supports the health and longevity of mealworms. Mealworms fed a combination of PS and rice bran prioritized consuming rice bran first, utilizing its essential nutrients for survival and growth before ingesting PS as a supplemental component (Yang et al. 2018; Peng et al. 2020).

Body weight measurements of mealworms from three diet groups over 28 days disclosed distinct differences in growth. Mealworms exclusively fed on rice bran had the highest body weight, with an average of 58.60 mg. The PS+RB diet resulted in an average body weight of 32.30 mg, while the lowest body weight was observed in mealworms fed with PS, averaging 25.85 mg (Figure 1.B). PS lacks nutrients and contains aromatic hydrocarbons that are difficult for mealworms to absorb, making the PS diet insufficient to promote healthy growth. Analysis of Variance (ANOVA) revealed substantial differences ($p<0.05$) in body weight between mealworms fed the RB diet and those fed PS1 and PS+RB diets. These findings had significant had significant implications for the development of optimal mealworm diets. However, the differences between the PS+RB and PS1 diet groups were not significant.

Metagenomic analysis of gut microbiome

The impact of PS diet on gut microbiome composition

The metagenomic analysis of the mealworm gut microbiome, following 28 days of PS1 or RB1 diet treatments, provides a deepened understanding of microbial ecology and biodiversity in response to dietary shifts. The sequencing data revealed that the PS1 diet sample generated 13,505,003 reads, while the RB1 diet sample produced 13,982,775 reads. Taxonomic analysis showed distinct differences in prokaryote composition between the two diet groups. The RB1 diet group exhibited higher diversity at higher taxonomic levels, with 96 phyla and 71 classes, compared to the PS1 diet group's 66 phyla and 69 classes. At the order level, RB1 also had more bacterial orders (139) than PS1 (133). However, at the family level, both groups showed comparable microbial diversity, with 231 families in RB1 and 233 in PS1, suggesting a leveling of diversity at finer taxonomic resolutions.

The data on gut microbiome composition are presented in Figure 2, which illustrates the abundance of prokaryotes within the mealworm gut. Proteobacteria were the most dominant phylum in both groups (Figure 2.A).

Proteobacteria constituted 53.67% of the gut microbiota in the RB1 diet and 53.87% in the PS1 diet. This dominance is consistent with their crucial ecological role. Proteobacteria represent a highly diverse microbial phylum comprising genera such as *Pseudomonas, Cupriavidus, Burkholderia*, and *Alcaligenes*, which are widely recognized for their roles in biodegrading synthetic plastics, including polystyrene (Hou and Majumder 2021). These bacteria inhabit various natural and anthropogenic niches ranging from water and sediment to plastic-contaminated environments like mangrove sediments, marine biofilms, and insect guts (Terova et al. 2021; Zhang et al. 2024), where their enzymatic systems, including cytochrome P450, monooxygenases, and ring-hydroxylating dioxygenases, facilitate the breakdown of carbon-carbon bonds and aromatic structures in polymer chains (Terova et al. 2021; Zhang et al. 2024). Their metabolic versatility and environmental adaptability position Proteobacteria as promising agents for microbial-based plastic bioremediation strategies.

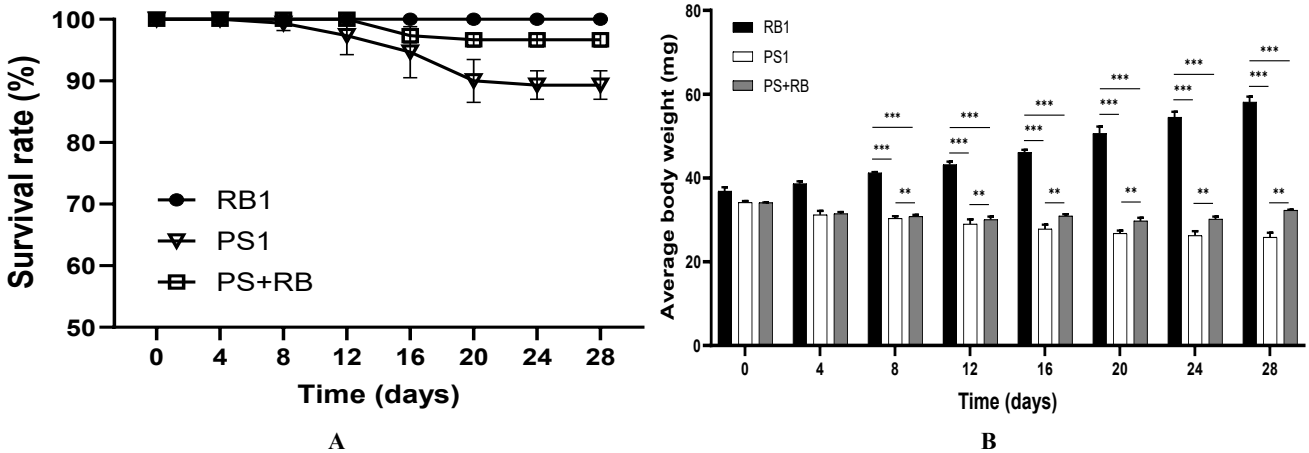

Figure 1. Survival and growth of mealworms during treatment: A. The survival rate of mealworms, B. The weight of mealworms (All values represent mean±SD, n = 3. Symbol *** above the line represents significant differences ($p<0.05$) among treatments for each feed based on the one-way ANOVA test

Figure 2.B presents a heatmap of the 15 most abundant gut bacterial phyla in larval groups fed with RB1 and PS1 diets. Proteobacteria dominated both dietary groups, with the highest relative abundance observed in the RB1-fed larvae. Other phyla, such as Actinobacteria, Aquificae and Bacteroideted exhibited relatively similar distributions across diets, while Cyanobacteria, Verrucomicrobia, and Planctomycetes showed minor variations in abundance. These compositional patterns suggest that dietary input plays a pivotal role in shaping gut microbial structure, with RB1 potentially promoting a more Proteobacteria-enriched environment. The presence of diverse phyla across both diets highlights the ecological plasticity of the larval gut microbiome. Comparative insights into phylum-level shifts may reflect functional adaptations to nutrient availability, supporting broader linkages between microbial diversity and host ecological resilience.

Despite the consistent dominance of Proteobacteria in mealworms, variations in gut microbiota composition in response to a PS diet have been documented across different insect species. For instance, Lou et al. (2020) identified Firmicutes and Proteobacteria as the dominant phyla in *G. mellonella* under PS diet conditions, whereas Quan et al. (2023) observed a predominance of Tenericutes (47.27%) followed by Proteobacteria (19.99%) in *Z. atratus* subjected to a similar diet. Additionally, Urbanek et al. (2024) reported that Proteobacteria and Firmicutes were the dominant phyla in *Z. morio* fed with PS, further highlighting the variability in microbial responses across different species. Beyond Proteobacteria, the three most abundant phyla were Actinobacteria (RB1 6.77%; PS1 6.44%), Aquaficae (RB1 6.48%; PS1 6.42%), and Bacteriodetes (RB1 6.45%; 6.05%). The similarity in phylum abundance across diet treatments underscores the resilience and adaptability of the mealworm gut microbiome. Despite drastic differences in dietary substrates, the gut ecosystem maintained a relatively stable microbial composition, emphasizing the microbiome's central role in the survival and digestion of mealworms across varied environments.

The top three most abundant bacterial families in RB1 and PS1 diet groups are illustrated in Figure 2.C. The Aquificaceae family dominated both groups, with the highest relative abundance in the RB1 diet group (15.52%). In comparison, in the PS1 diet group, Aquificaceae remained the most dominant, but with a slightly lower percentage (15.17%). Aquificaceae are thermophilic bacteria commonly found in extreme environments such as hot springs. (Fortunato et al. 2018). Their presence in the mealworm gut suggests the adaptation of the microbiome to specific gut conditions.

The Burkholderiaceae family was present in both the RB1 diet group (4.51%) and PS1 diet group (3.94%). This presence indicates their potential functional role across diverse dietary environments. This bacterial family plays a crucial role in degrading aromatic compounds (Yadav et al. 2021).

Figure 2.D displays the heatmap of the 15 most abundant gut bacterial families in mealworm groups fed with RB1 (Rice Bran) and PS1 (Polystyrene) diets. Aquificaceae and Streptococcaceae were predominant across both diets, with notably high relative abundances. Families such as Erwiniaceae and Burkholderiaceae also showed substantial representation, while Roseobacteraceae and Marinilabiliaceae were less abundant. These patterns underscore the influence of dietary substrates on gut microbial family composition, reflecting distinct ecological niches shaped by nutrient availability.

The genus-level composition of gut microbiota, as presented in Figure 2.E, revealed a predominance of *Glycocaulis* in both RB1 and PS1 samples, with relative abundances of 17.55% and 16.43%, respectively, followed by *Alteriqipengyuania* (RB1: 13.31%; PS1: 13.15%). Notably, *Rhodopirellula* exhibited a marked increase in the PS1 group (3.82%) compared to RB1 (1.30%), while *Nocardioides,* a genus known for hydrocarbon and aromatic compound degradation (Mitzscherling et al. 2022; Brzeszcz et al. 2024), showed a modest rise from 2.15% (RB1) to 2.67% (PS1), suggesting its potential role in PS biodegradation. These findings diverge from prior studies across insect models.

For instance, Lou et al. (2020) observed *Enterococcus* dominance in *G. mellonella* fed PS, while Lou et al. (2021) reported enrichment of *Enterococcus* and unclassified Enterobacteriaceae in the PS diet of the PS diet of *Z. atratus*. Similarly, Quan et al. (2023) identified *Spiroplasma* and unclassified Enterobacteriaceae as prevalent genera under PS diets. Contrastingly, Urbanek et al. (2024) documented *Klebsiella, Morganella*, and *Chryseobacterium* as dominant genera in *Z. morio* consuming PS, highlighting host-specific microbial adaptations. Such disparities likely reflect interspecies baseline differences, environmental factors, and experimental variables.

Figure 2.F presents the heatmap of the 15 most abundant gut bacterial genera in larval groups fed with RB1 (Rice Bran) and PS1 (Polystyrene) diets. The genus-level profiles reveal distinct microbial assemblages shaped by dietary input. Genera such as *Candidatus*, *Thioglobus*, *Aquifex*, and *Streptococcus* were more prevalent in the RB1-fed larvae, suggesting an enrichment of taxa associated with fermentative and sulfur-related metabolic pathways. In contrast, *Spiroplasma* and *Fluviispira* dominated the PS1 group, potentially reflecting microbial adaptation to synthetic polymer degradation.

At the genus level, RB1 diet group contained 329 genera, while the PS1 diet group consisted of 334 genera (Figure 2.G). Among these, 88 genera were unique to the RB1 diet group, while 93 were exclusive to the PS1 diet group. The majority of genera detected through metagenomic analysis were associated with the degradation of hydrocarbons and organic compounds, and were identified for the first time using this approach. Notably, nine genera identified in the PS1 diet group exhibited distinct metabolic versatility. *Oceanobacter*, *Henriciella*, and *Maribacter* are known for their ability to degrade polyaromatic hydrocarbons (Teramoto et al. 2009; Atanasova et al. 2021; Ridley et al. 2024). In addition, *Burkholderia* specializes in naphthalene degradation (Mohapatra and Phale 2021), while Dyadobacter is adept at hydrocarbon degradation (Olowomofe et al. 2019). Further highlighting the biodegradation potential,

Saccharomonospora possesses cutinase enzymes that facilitate PET plastic degradation (Purohit et al. 2020). Eubacterium is recognized for its fiber-digesting abilities (Ladino-Orjuela et al. 2016) and *Ferroglobus* is capable of anaerobically degrading aromatic compounds (Castro et al. 2022). Furthermore, *Tsuneonella* has been associated with oil sludge bioremediation (Sun et al. 2021). Collectively, these genera highlight the metabolic adaptability of the mealworm gut microbiota when exposed to a PS-rich diet, emphasizing their potential role in nutrient cycling and biodegradation processes.

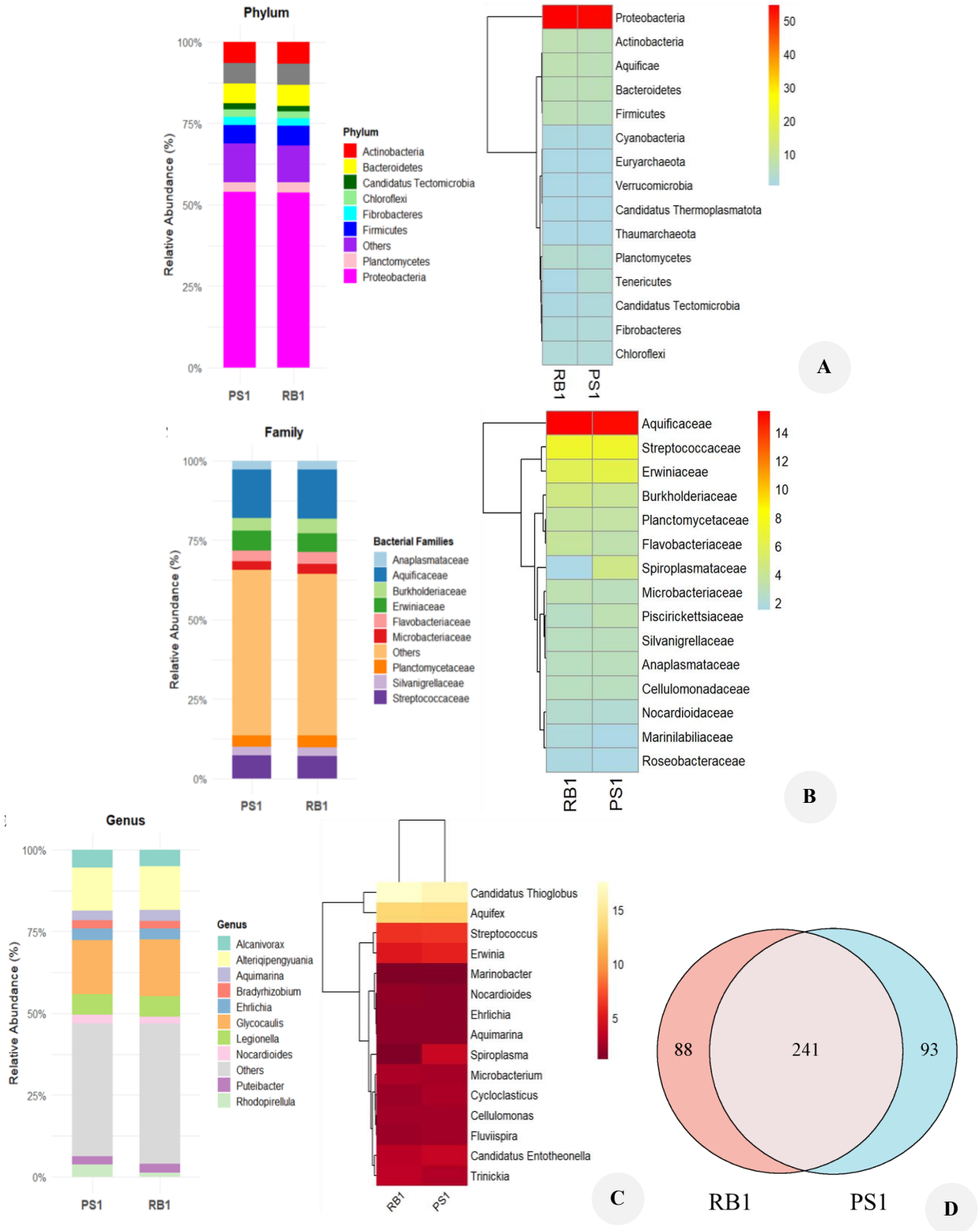

Figure 2. Comparison of the relative abundance of gut microbiome. A. phylum, B. family, C. genera, D. Venn diagram

The gut microbiome of mealworm under a PS diet exhibited a distinctive community structure, marked by the enrichment of low-abundance and metabolically specialized genera such as *Oceanobacter*, *Henriciella*, and *Tsuneonella* taxa absent from the rice bran diet group. These microorganisms are recognized for their roles in degrading aromatic hydrocarbons and mediating bioremediation in challenging environments, indicating a microbial shift tailored to xenobiotic exposure. Their occurrence, alongside an upregulation of degradation-related genes, suggests the presence of underexplored microbial lineages with unique enzymatic capabilities. This points to the insect gut as a valuable microhabitat for discovering functional consortia with potential for synthetic polymer degradation.

This study highlights the ecological value of gut symbionts in insects, particularly mealworms, as crucial sources of diverse microbes with potential biotechnological applications. This symbiotic relationship is synergistic: the physical action of the insect facilitates microbial access to the plastic material, while the enzymatic activity of the microbes enables more thorough degradation (Bilal et al. 2021). The increased presence of hydrocarbon-degrading bacteria, such as *Burkholderia*, *Oceanobacter*, and *Nocardioides*, in the gut of mealworms fed a PS diet indicates that these symbiotic communities can adapt to synthetic materials (Dar et al. 2024). This demonstrates the metabolic flexibility of the gut microbiota under chemical stress and suggests that insect guts may be valuable environments for discovering novel degradation pathways. As global attention shifts towards sustainable plastic waste management, preserving and studying these adaptable symbiotic microbiomes is essential for understanding microbial resilience and ecological adaptation in polluted ecosystems.

The metagenomic analysis revealed several novel and functionally significant taxa in the PS1 diet group, including *Oceanobacter, Henriciella, Maribacter*, and *Tsuneonella*, which were either absent or rare in the RB1 group. These genera are known for their specialized roles in degrading Polyaromatic Hydrocarbons (PAHs) and other recalcitrant compounds, suggesting their adaptive recruitment under PS dietary stress. Notably, *Nocardioides* and *Burkholderia* exhibited increased abundance in the PS1 group, corroborating their established functions in hydrocarbon and naphthalene degradation. The presence of *Saccharomonospora*, a genus encoding cutinase enzymes for PET degradation, a genus encoding cutinase enzymes for PET degradation, further highlights the gut microbiome's potential for plastic biodegradation. These findings underscore the mealworm gut as a reservoir of novel microbial taxa with tailored metabolic capabilities for xenobiotic degradation, offering promising candidates for bioremediation applications. The enrichment of low-abundance, specialized genera emphasizes the microbiome's dynamic response to synthetic polymer diets and its ecological versatility.

The presence of *Nocardioides* and *Burkholderia* indicates that the mealworm gut ecosystem is not merely a site of microbial colonization, but also a space for functional adaptive selection. *Nocardioides*, a specialized actinomycete, has been shown to degrade various aromatic and complex polymer compounds even in nutrient-poor environments (Ma et al. 2023). *Burkholderia*, on the other hand, demonstrates remarkable genomic and metabolic flexibility, enabling it to adapt to xenobiotic stress while contributing to nutrient cycling and detoxification (Mannaa et al. 2019; dos Santos et al. 2021). These adaptations reinforce the view that the insect gut is a microhabitat rich in functional biodiversity, with microbial communities diverse not only in taxonomy but also in metabolism and ecological roles (Haider et al. 2025). Therefore, the mealworm gut acts as a microbial bioprospecting hotspot for the development of sustainable plastic biodegradation strategies grounded in ecological function

The gut microbiome of mealworms fed with PS exhibited a distinctive community structure enriched with metabolically versatile genera such as *Burkholderia, Oceanobacter*, and *Tsuneonella*, which are known for their roles in degrading aromatic hydrocarbons and facilitating bioremediation in challenging environments. This functional biodiversity reflects the microbiome's ecological adaptability under xenobiotic stress and highlights its potential contribution to microbial ecosystem services, particularly in nutrient cycling and plastic waste degradation. Recent studies have emphasized that insect gut microbiota harbor specialized enzymatic systems capable of depolymerizing synthetic polymers into assimilable intermediates, with enhanced degradation efficacy observed in microbial consortia rather than isolated strains. For instance, Xu et al. (2024) reviewed the capacity of gut microbes from *T. molitor, G. mellonella*, and *Z. atratus* to degrade polystyrene through synergistic enzymatic pathways. Similarly, De Filippis et al. (2023) demonstrated that plastic-containing diets significantly reshape the gut microbiome of *Hermetia illucens*, enriching genes encoding DyP-type peroxidases and alkane monooxygenases involved in polymer degradation. These findings underscore the insect gut as a promising reservoir of microbial diversity and functional genes for developing sustainable biodegradation strategies. By leveraging the metabolic flexibility of these symbiotic communities, mealworms may serve as a model system for advancing microbe-based plastic waste management technologies.

Recent advances in metagenomic approaches have significantly expanded our understanding of microbial functional diversity within insect gut ecosystems, positioning them as promising targets for ecological bioprospecting. Kaltenpoth et al. (2025) emphasized that beneficial bacterial symbionts in insects contribute to host fitness through nutrient provisioning, detoxification, and enzymatic degradation of recalcitrant compounds, underscoring their biotechnological relevance in waste management and bioremediation. Ramond et al. (2025) proposed a unified framework for assessing microbial functional diversity and redundancy, highlighting the role of symbiotic microbes in maintaining ecosystem resilience under environmental stress. Moreover, Fan et al. (2025) demonstrated that microbial communities in contaminated aquifers retain functional gene diversity despite taxonomic shifts, suggesting that functional traits are selectively maintained

under xenobiotic pressure. These findings collectively support the notion that insect-associated microbiomes harbor metabolically robust and ecologically adaptable taxa, which can be harnessed for sustainable biodegradation strategies and the discovery of novel enzymatic pathways.

Index diversity of bacteria

Table 2 describes the diversity indices of bacteria found in the samples. The Shannon Index (1.90-1.95) indicates moderate diversity for phylum, with evenness (0.45-0.47) being low. This suggests an uneven distribution of species, with a few dominating while others are less abundant. The low dominance (0.31-0.32) means no single species is dominant in this category. For class, the Shannon Index (2.37-2.38) also reflects moderate diversity. While evenness (0.56) remains low, showing an uneven distribution of species, the low dominance (0.19) suggests that no species is overwhelmingly dominant. Moving to order, the Shannon Index (3.61-3.62) shows moderate diversity, but evenness (0.73-0.74) is high, indicating a more balanced species distribution. With dominance (0.04-0.05) being very low, this suggests a high level of diversity with no dominant species. In the case of family, the Shannon Index (3.89) indicates high diversity, and evenness is perfect at 1.00 for RB1. At the same time, At the same time, PS1 shows moderate evenness (0.71), pointing to a more even distribution in RB1 and a bit more dominance in PS1. Dominance (0.05) remains low, indicating no single species dominates. For the genus, the Shannon Index (3.79-3.81) suggests high diversity, though evenness (0.66-0.65) is low, showing an uneven distribution with a few dominant genera. The low dominance (0.06) still indicates some balance in the overall distribution. At the species level, the Shannon Index (4.38-4.39) reflects very high diversity, with evenness (0.67) still on the lower side, meaning species are not evenly distributed. Dominance is again very low (0.03-0.04), suggesting a large number of species contribute to the diversity, without any one species being dominant.

The highest diversity is observed at the species level, the spesies level, although evenness remains low, particularly in PS1, indicating some imbalance in the microbial community of the mealworm gut. Diversity and distribution are generally lower at the phylum and class levels, the phylum and class levels, but both order and family show more even distribution and higher diversity. Genus and species show very high diversity, although distribution among species remains uneven. This ecological balance is a key indicator of the community's ability to maintain ecosystem functions amid drastic environmental changes (Lozupone et al. 2012; Maron et al. 2018). Overall, both diets (RB1 and PS1) produced similar microbiome diversity patterns, with minor variations in Evenness and Dominance values. This pattern reflects a dynamic and flexible ecosystem, where microbial communities can adapt to xenobiotic stress without losing functional diversity. Studies have shown that while environmental stress may reduce taxonomic diversity, functional diversity often remains intact through redundancy and adaptive selection mechanisms (Fan et al. 2025; Ramond et al. 2025). The resulting community is not merely a taxonomic response, but a reflection of ecological function-based selection such as the degradation of aromatic compounds, polymer metabolism, and detoxification of foreign substrates (Sharma and Dubey 2021; Miglani et al. 2022).

Functional gene analysis of the mealworm gut microbiome: A comparison between PS and rice bran diets

Based on the KEGG database (Figure 3), the functional genes of the mealworm gut microbiome were categorized into six major pathways: organismal systems, metabolism, human diseases, genetic information processing, environmental information processing, and cellular processes (Table 3). Among these, metabolism was the predominant pathway in both RB1 and PS1 diet groups, accounting for 16.66% and 17.42%, respectively. The diversity of the most prevalent pathways within the metabolism category such as glucose metabolism, followed by lipid metabolism, cofactor and vitamin metabolism, the production of various secondary metabolites, and xenobiotic metabolism.

Table 2. Diversity index of bacteria in the mealworm gut

Taxonomic level	Shannon Index		Evenness		Dominance	
	RB1	PS1	RB1	PS1	RB1	PS1
Phylum	1.90	1.95	0.45	0.47	0.32	0.31
Category	Moderate	Moderate	Low	Low	Low	Low
Class	2.37	2.38	0.56	0.56	0.19	0.19
Category	Moderate	Moderate	Low	Low	Low	Low
Order	3.62	3.61	0.73	0.74	0.05	0.04
Category	High	High	Low	Low	Low	Low
Family	3.91	3.89	1.00	0.71	0.05	0.05
Category	High	High	Moderate	Low	Low	Low
Genus	3.81	3.79	0.66	0.65	0.06	0.06
Category	High	High	Low	Low	Low	Low
Species	4.38	4.39	0.67	0.67	0.04	0.03
Category	High	High	Low	Low	Low	Low

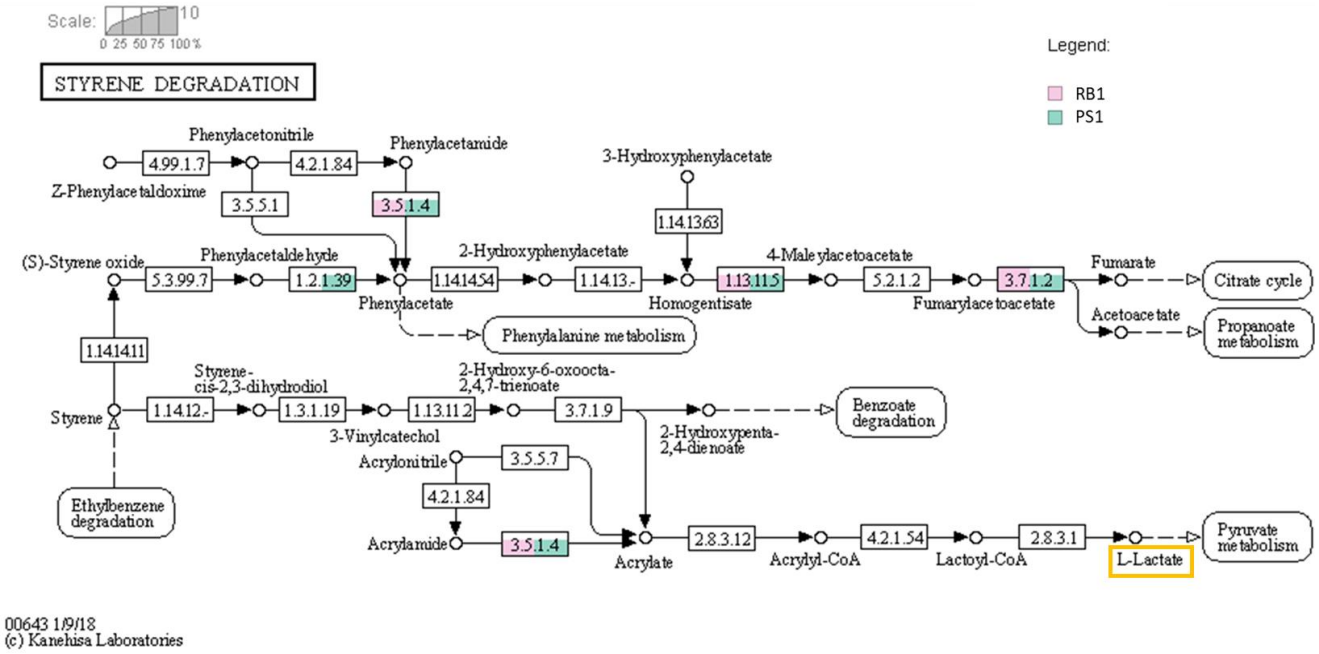

Figure 3. A KEGG pathway visualization produced by the MEGAN software (Huson et al. 2016), illustrating functional annotation of the gut microbiome metagenome from mealworm diet RB1 and PS1. Enzymes identified in the microbiota of the RB1 diet are highlighted in pink, while those from the PS1 diet are marked in green, Lactate, L-Lactat as an intermediate compound by an orange box

Based on the KEGG database, the functional genes of the mealworm gut microbiome were categorized into six major pathways: metabolism, genetic information processing, environmental information processing, cellular processes, organismal systems, and human diseases (Table 3). Among these, metabolism was the most represented category in both RB1 and PS1 groups, with relative abundances of 16.66% and 17.42%, respectively. This dominance of metabolism-related genes suggests that the gut microbiota plays a central role in supporting the host's digestive and metabolic functions. It reflects the importance of microbial communities in processing dietary components, synthesizing essential metabolites, and potentially contributing to host health. The slightly higher metabolic gene abundance in the PS1 group may indicate enhanced microbial metabolic activity in response to specific dietary or environmental factors. Furthermore, such enrichment could be linked to the production of bioactive metabolites, including antibacterial compounds, derived from microbial metabolic pathways.

The functional gene profile of the mealworm gut microbiome revealed the presence of diverse xenobiotic degradation pathways, including the breakdown of benzoate, styrene, chloroalkanes and chloroalkenes, toluene, and caprolactam, as well as drug metabolism mediated by cytochrome P450 and other enzymes (Table 4). This metabolic versatility is driven by a broad array of enzymes capable of transforming complex and persistent environmental pollutants. A comparative analysis between the RB1 and PS1 diet groups indicated a higher representation of xenobiotic degradation genes in the PS1 group. For instance, the proportion of genes involved in the degradation of chloroalkanes and chloroalkenes reached 8.38% in PS1, compared to 3.73% in RB1. Similarly, higher values were observed in the PS1 group for styrene (0.56% vs. 0.34%), steroid degradation (1.12% vs. 0.68%), and xenobiotic metabolism by cytochrome P450 enzymes (1.12% vs. 0%). These differences suggest that PS1-associated gut microbes may possess a greater enzymatic capacity for degrading halogenated and aromatic compounds. Such capabilities are important, as many of these compounds, especially aromatic hydrocarbons, are known for their persistence and toxicity in the environment (Yadav et al. 2021). The enrichment of cytochrome P450-mediated pathways also indicates the presence of oxidative mechanisms that play a key role in the initial activation and breakdown of xenobiotics.

Functional metagenomic analysis identified styrene degradation pathways in the gut microbiome of mealworms fed PS1 and RB1 diets. As summarized in Table 5, both diet groups harbored key enzymes involved in aromatic compound degradation, including homogentisate 1,2-dioxygenase (EC 1.13.11.5), amidase (EC 3.5.1.4), and fumarylacetoacetase (EC 3.7.1.2). Interestingly, phenylacetaldehyde dehydrogenase (EC 1.2.1.39) was detected exclusively in the PS1 group, suggesting that exposure to PS may induce or enrich specific enzymatic pathways linked to styrene detoxification. This enzyme catalyzes the oxidation of phenylacetaldehyde to phenylacetate, which is a key intermediate in aromatic metabolism. The identification of these enzymes highlights the metabolic flexibility of the mealworm gut microbiome in processing aromatic xenobiotics under both natural (RB) and plastic-rich (PS) conditions. This capacity may stem from the insect's adaptation to dietary lignocellulosic materials such as rice bran, which naturally contain aromatic heteropolymers (Rosado et al. 2021). However, several enzymes involved in the styrene degradation

pathway remain unidentified, suggesting that a complete elucidation of the pathway and confirmation of PS-to-styrene biotransformation will require further targeted studies beyond this metagenomic analysis.

The relative abundance of enzyme classes in the gut microbiome of mealworms fed PS (PS1) and rice bran (RB1) diets revealed distinct functional profiles (Table 6). Hydrolases were the most abundant enzyme class in both groups (PS1: 35.69%; RB1: 34.73%), followed by transferases (PS1: 21.33%; RB1: 20.18%) and oxidoreductases (PS1: 19.96%; RB1: 20.45%). These three enzyme classes—hydrolases, oxidoreductases, and transferases—play crucial roles in xenobiotic metabolism, particularly in the detoxification of persistent compounds by altering their chemical structure to improve solubility and reduce toxicity (Mesnage et al. 2018). The initial phase of aromatic compound degradation typically involves oxidation, often catalyzed by oxidoreductase enzymes such as monooxygenases (EC 1.14.13.-, EC 1.14.14.-) and dioxygenases (EC 1.13.11.-) (Ladino-Orjuela et al. 2016). Hydrolases, on the other hand, are essential in breaking ester or glycosidic bonds, contributing to the further breakdown of complex xenobiotic structures. Several microbial enzymes, including cytochrome P450, laccase, cellulase, phytase, protease, and lipase, have been implicated in the degradation of aromatic and plastic-related compounds. These enzymes reflect the diverse enzymatic toolkit used by the gut microbiota for environmental detoxification (Miglani et al. 2022). The relative distribution of these CAZy enzyme classes in both RB1 and PS1 diets underscores the metabolic versatility of the mealworm gut microbiome and its potential application in biotransformation and bioremediation of aromatic and plastic-derived pollutants.

Table 7 highlights the presence of various enzymes involved in PS degradation, including monooxygenases and cytochrome P450s, which are capable of incorporating molecular oxygen and catalyzing oxidative reactions on organic compounds. These enzymes were predominantly found in the RB1 diet group (124 enzymes), slightly higher than in the PS1 group (122 enzymes), suggesting their potential role in the initial oxidation of PS. Previous studies have shown that the monooxygenase StyA/StyB plays a critical role in the styrene degradation pathway in *Gordonia rubripertincta* CWB2 (Lienkamp et al. 2021).

Similarly, Venegas et al. (2024) identified flavin-binding monooxygenase and three cytochrome P450s as key enzyme candidates in the PS degradation system of *G. mellonella*. Although these enzymes shared low sequence identity with bacterial enzymes such as StyA and StyA2B, they exhibited notable oxidative activity, suggesting the existence of a distinct degradation mechanism in eukaryotes. This cross-kingdom comparison underscores the functional diversity of monooxygenases and highlights potential evolutionary adaptations for utilizing aromatic substrates like PS.

Superoxide dismutase (Fe-Mn), although discovered in smaller quantities in both diet groups, was more prevalent in the RB1 diet group with 7 enzymes than in the PS1 diet group with 5 enzymes. This enzyme is crucial in oxidizing side chains or cleaving C-C bonds in PS and lignin, potentially converting PS polymers into aromatic residues. Despite being less abundant than cytochrome P450, enzymes such as alkylglycerol monooxygenase (AGMO), aldehyde dehydrogenase (ALDH), and peroxidase play key roles in aromatic ring cleavage, generating intermediate products. Aldehyde dehydrogenase (ALDH; EC:1.2.1.3) catalyzes the oxidation of both aromatic and medium-chain aliphatic aldehydes, common intermediates in xenobiotic metabolism, and less reactive and more readily excreted carboxylic acids (Vasiliou et al. 2000).

Additionally, the PS1 group exhibited a higher abundance of aldehyde dehydrogenase (ALDH; EC:1.2.1.3), which oxidizes aromatic aldehydes into less toxic carboxylic acids, suggesting an adaptive response to PS degradation. Notably, alkylglycerol monooxygenase (AGMO; EC:1.14.16.5) and superoxide dismutase (Fe-Mn; EC:1.15.1.1) were also identified as novel contributors to aromatic ring cleavage, despite their lower abundance. These findings highlight the metabolic versatility of the mealworm gut microbiome, particularly under PS-exposed conditions, and underscore the potential of these enzymes in bioremediation applications. Further characterization of their catalytic mechanisms and substrate specificity is warranted to fully exploit their biodegradation potential. On the other hand, long-chain fatty acid-CoA ligase (ACSL) was slightly more abundant in the PS1 diet group (57 enzymes) than in the RB1 diet group (54 enzymes) despite its high presence in both diet groups. This enzyme plays a key role in hydrolyzing intermediate products into long-chain fatty acids, further highlighting the potential utilization of PS degradation products.

Table 3. Relative abundance of KEGG metabolism function

KEGG functions	RB1 (%)	PS1 (%)
Metabolism	16.66	17.42
Genetic information processing	3.29	3.40
Environmental information processing	8.10	7.77
Cellular processes	5.05	5.01
Organismal systems	8.71	8.29
Human diseases	8.51	8.40
Brite hierarchy	43.50	43.65
Not included in pathway or brite	6.18	6.05

Table 4. Xenobiotic degradation

KEGG pathways	Percent of genes	
	RB1	PS1
Benzoate degradation	3.73	3.63
Aminobenzoate degradation	6.44	6.70
Chloroalkane and chloroalkene degradation	3.73	8.38
Toluene degradation	1.02	1.40
Ethylbenzene degradation	0.34	0.28
Styrene degradation	0.34	0.56
Caprolactam degradation	1.36	1.12
Naphthalene degradation	9.15	9.78
Steroid degradation	0.68	1.12
Xenobiotic metabolism by cytochrome P450	0.00	1.12
Drug metabolism by cytochrome P450	17.63	18.16
Xenobiotic drug metabolism by other enzymes	13.90	15.36

Table 5. Annotation of aromatic xenobiotic biodegradation enzymes from the functional genes of the gut microbiome of *T. molitor* based on the KEGG database

Enzyme	Total enzyme detected in the mealworm gut		Xenobiotic degradation pathway
	PS1	RB1	
Phenylacetaldehyde dehydrogenase [1.2.1.39]	1	0	Styrene
Amidase [3.5.1.4]	1	1	Styrene
Homogentisate 1,2-dioxygenase [1.13.11.5]	1	1	Styrene
Fumarylacetoacetase [3.7.1.2]	2	2	Styrene
3-hydroxyacyl-CoA dehydrogenase [1.1.1.35]	1	1	Toluene

Table 6. Relative abundance of CaZy enzyme in the mealworm gut microbiome

Enzymes	Percent of sequences	
	RB1	PS1
Oxidoreductase	20.45	19.96
Transferase	20.18	21.33
Hydrolase	34.73	35.69
Lyase	3.36	3.16
Isomerase	2.10	2.16
Ligase	6.06	5.75
Translocase	13.12	11.96

Table 7. Potential enzymes involved in PS degradation

Representative enzymes	Mode of action	Total enzyme detected in the mealworm gut		References
		RB1	PS1	
Cytochrome P450 [EC:1.14.-.-]	Introducing one atom of molecular oxygen into unactivated C-H bonds	124	122	(Hou and Majumder 2021)
Monooxygenase [EC 1.14.13.-]	Catalyzing hydroxylation, sulfoxidation, heteroatom oxygenation, N-hydroxylation, and oxidative decarboxylation	6	5	(Ladino-Orjuela et al. 2016)
Monooxygenase [EC 1.14.14.-]	Catalyzing hydroxylation, sulfoxidation, oxidation, epoxidation, and desulfurization	124	122	(Ladino-Orjuela et al. 2016)
Superoxide dismutase (Fe-Mn) family [SOD; EC:1.15.1.1]	Oxidizing side chains or cleaving C-C bonds of PS and lignin, converting the PS polymer into aromatic residues	7	5	(Mamtimin et al. 2023)
Alkylglycerol monooxygenase [AGMO; EC:1.14.16.5]	Cleaving aromatic rings and converting them into intermediate products	1	1	(Mamtimin et al. 2023)
Aldehyde dehydrogenase family [ALDH; EC:1.2.1.3]	Cleaving aromatic rings and converting them into intermediate products	9	27	(Mamtimin et al. 2023)
Peroxidase [PO; EC:1.11.1.7]	Cleaving aromatic rings and converting them into intermediate products	12	12	(Mamtimin et al. 2023)
Long-chain-fatty-acid-CoA ligase [ACSL; EC:6.2.1.3]	Hydrolyzing intermediate products to generate long-chain fatty acids	54	57	(Mamtimin et al. 2023)
Carboxyl esterase [CE10; EC 3.1.1.3]	Cleaving aromatic rings and converting them into intermediate products	32	35	(Mamtimin et al. 2023)
Lipase [CE1; EC 3.1.1.-]	Cleaving aromatic rings and converting them into intermediate products	40	33	(Mamtimin et al. 2023)

Comparison of PS degradation in mealworm gut and BH liquid medium

Figure 4.A illustrates a consistent decline in PS weight over 28 days, indicating progressive PS degradation by mealworms. Mealworms can consume various types of plastics, including polyvinyl chloride, polyethylene, and polypropylene, through the strong mandibular activity that enables them to chew these materials (Yang et al. 2015; Urbanek et al. 2020). The biodegradation of PS in the mealworm gut involves a mechanical process of plastic fragmentation, which increases area, and a biological process mediated by bioemulsion secretion to enhance polymer degradation (Lou et al. 2021; Wang et al. 2022). The gut microbiota then secretes extracellular enzymes that catalyze the depolymerization of PS fragments into small molecules, which can subsequently be mineralized into CO_2 or assimilated into biomass. At the same time, At the

same time, undigested residues are excreted with gut microbes via frass for further degradation (Yang et al. 2015).

Both treatment groups, PS1 (PS only) and PS+RB (PS with rice bran), exhibited a gradual increase in PS weight loss over time. However, the T-test analysis revealed no substantial differences in PS consumption between the two groups (p-value<0.05) at any measured time point. On day 28, the PS1 diet group caused a PS weight loss of 6.38%, which was higher than the 6.11% observed in the PS+RB diet group (Figure 4.A). This finding indicates that incorporating rice bran does not improve the degradation of PS. A possible explanation is that rice bran, rich in easier-to-digest nutrients such as carbohydrates, proteins, and fats, may divert the feeding preference of mealworms away from PS. Furthermore, rice bran may fulfill their basic energy needs, potentially reducing the necessity to consume PS. This, coupled with its potential to alter the gut microbiome composition in a manner that diminishes the efficiency of PS degradation. This aligns with their natural feeding preference for organic materials over synthetic polymers. These findings differ from previous research (Brandon et al. 2018; Wang et al. 2024) reporting that co-diets supplemented with organic matter enhanced plastic degradation. This discrepancy may be attributed to variations in experimental conditions, such as differences in co-diet composition, mealworm strains, or microbial communities involved in plastic degradation (Pham et al. 2023).

The degradation of powdered PS by the gut microbiome consortium in BH liquid medium exhibited an increasing trend in PS weight loss at four-day intervals (Figure 4.B). However, this reduction remained lower compared to the degradation by mealworms. At the end of the 28-day observation period, PS degradation in the BH liquid medium reached 3.49%, while PS weight loss in the PS1 diet group was 6.38% and 6.11% in the PS+RB diet group. The higher PS degradation in the mealworm gut is attributed to the presence of bioemulsifying factors that facilitate PS degradation within the gut (Lou et al. 2021; Pivato et al. 2022).

Comparative analysis of gut bacteria in mealworms and BH liquid medium

The quantity of intestinal bacteria in the mealworm gut before and after treatment is influenced by diet composition (Figure 4.B). In the PS diet group, total bacterial counts decreased substantially from 6.13 log CFU/mL on day 0 to 4.10 log CFU/mL on day 28, with the reduction being statistically significant (p-value<0.05). This sharp decline suggests a selective pressure imposed by the PS-rich environment, wherein only specific bacterial taxa capable of PS degradation survive and proliferate. The hydrophobic and recalcitrant nature of PS may create a hostile gut environment for most mealworm gut bacteria by altering pH, nutrient availability, or other environmental factors critical for bacterial growth. In contrast, the PS+RB diet group exhibited no considerable differences in the TPC of gut bacteria over the 28-day treatment, remaining stable at 6.26 log CFU/mL. This stability indicates that the addition of rice bran as the co-diet provided sufficient nutrients to support the gut bacterial population.

The TPC data of bacteria in the gut versus in BH liquid medium can be observed in Figure 4.B. Although the percentage of PS weight reduction in BH liquid medium was lower compared to that achieved by mealworms over the same 28-day period, the bacteria TPC in the liquid culture were significantly higher than those of culturable gut bacteria. On day 28, the bacterial count in BH liquid medium reached 9.42 log CFU/mL, compared to 6.37 log CFU/mL in the RB diet group and 6.26 log CFU/mL in the PS+RB diet group. It suggests the presence of a substantial number of non-culturable microorganisms in the mealworm gut that may contribute to PS degradation within the gut. The high TPC of bacteria in the liquid medium (9.42 log CFU/mL on day 28) highlights the strong metabolic adaptability of the microbial consortium under nutrient-limited conditions. Gut microbes demonstrate high resilience in a liquid medium with minimal salt content, utilizing PS as the sole carbon source.

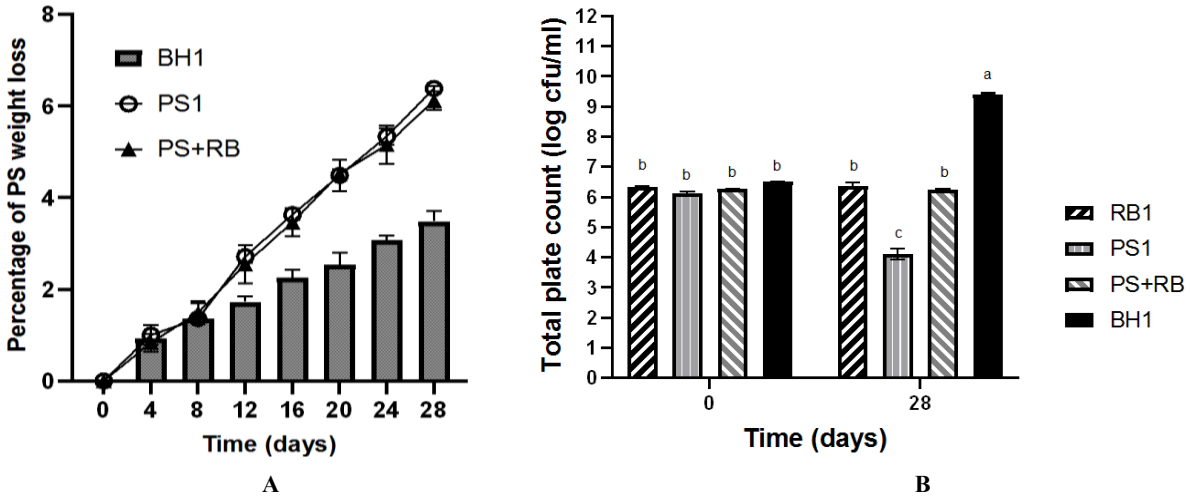

Figure 4. A. PS degradation by mealworm gut activity and gut microbiota consortia in Bushnell Haas (BH1) liquid medium. Error bars represent±SD (n = 3). A. Significant differences were determined by a t-test (p-value<0.05), B. Bacterial count dynamics in the mealworm's gut and Bushnell Haas Broth (BH1) on days 0 and 28. Error bars represent±SD (n = 3). Different letters above the bars indicate significant differences among treatments within each diet, based on one-way ANOVA (p<0.05)

FTIR analysis of PS degradation during mealworm digestion

FTIR, a widely applied method in studies on plastic biodegradation (Wang et al. 2024), was employed to monitor changes in the functional groups of PS following 28 days of mealworm digestion. FTIR spectra show the differences between PS frass and virgin PS foam (Figure 5.A). A new C=C bending group at 879 cm^{-1} was observed in PS frass but absent in PS control, indicating the formation of new functional groups during digestion. Furthermore, the intensity of the benzene-associated C=C bending group at 696 cm^{-1} declined in PS frass, suggesting a decrease in benzene content after gut passage. The PS+RB frass spectrum revealed the loss of the C=C benzene group at 696 cm^{-1} and the C-O-O-C group at 1029 cm^{-1}, implying enhanced PS oxidation and biodegradability due to the inclusion of rice bran. Despite differences in spectra, both PS and RB diet groups contained C-H groups in the aromatic structure at 876 cm^{-1}. Notably, the FTIR spectrum in the RB1 diet group revealed new C-H bending at 1644 cm^{-1}, which was absent in the virgin RB spectrum (Figure 5.B).

Metabolic profiling of PS degradation

Heatmap and PCA analysis of metabolites in mealworm frass

The collected frass samples from each treatment were tested using GC-MS to identify metabolic by-products. The analysis verified a range of compounds, including alkanes, alkenes, acids, alcohols, antioxidants, and aromatic hydrocarbons. Frass from the RB1 diet revealed an absence or low abundance of benzene and glycolic acid compounds (Figure 6.A). However, frass from the PS+RB diet lacked the following compounds: oleic acid, phthalic acid, di(2-propylpentyl) ester, 2,4-Di-tert-butylphenoxytrimethyl-silane, and 2,6-Bis(tert-butyl) phenol.

The GC-MS analysis of frass from three diet groups annotated substances, including alcohols, aromatic compounds, acids and fatty acids, and plastic additives (plasticizers). No styrene compounds were observed, in contrast to the findings of Tsochatzis et al. (2021a), who reported the presence of styrene monomer and styrene trimer in the mealworm body extracts after seven days of feeding on the PS diet. Although styrene was not discovered, benzene and benzyl alcohol, aromatic molecules that contribute to toluene degradation, were identified. It suggests that PS may be degraded into toluene and intermediate chemicals through toluene degradation. Other chemicals discovered include 1,2-butanediol and bis(2-ethylhexyl) phthalate, common plasticizers added to enhance flexibility.

Certain fatty acids were identified in the frass, including saturated fatty acids such as stearic acid, octanoic acid, palmitic acid, oleic acid, pentanoic acid, and unsaturated fatty acids (11-octadecenoic acid). These findings align with Son et al. (2020) and Tsochatzis et al. (2021b). Notably, stearic acid and palmitic acid were detected in all three diet groups. These fatty acids can be generated through the enzyme-mediated degradation of triacylglycerols and fatty acid metabolism in the insect gut microbiome (Tsochatzis et al. 2021b).

Lactic acid, glycolic acid, and 2-hydroxybutyric acid were among the acidic compounds discovered. Hydroxybutyric acid is associated with propanoate metabolism, while glycolic acid is a 2-hydroxy monocarboxylic acid structurally related to acetic acid, playing a role in glyoxylate and dicarboxylate metabolism. Glycolic acid functions as both a primary alcohol and a metabolite, and is known for its keratolytic properties. It also serves as the conjugate acid of glycolate.

Figure 6.B presents a Principal Component Analysis (PCA) biplot of mealworm frassfrass. PCA revealed that frass exposed to PS exhibited a significantly different metabolite profile compared to other treatments, with aromatic compounds, phenolics, esters, and fatty acids being the dominant components. The detection of compounds such as benzene, benzyl alcohol, and 2,6-bis(tert-butyl)phenol suggests the occurrence of styrene degradation, the main component of polystyrene, through microbial activity. These compounds have been widely reported as intermediate or end products of plastic biodegradation by microorganisms such as *Pseudomonas putida* and *Aspergillus niger* (Hahladakis et al. 2018). Additionally, metabolites like 1,2-butanediol and 2-hydroxybutyric acid indicate fermentative activity by microbes utilizing synthetic polymers as carbon sources (Pathak and Navneet 2017). The presence of long-chain fatty acids, including stearic acid and 11-octadecenoic acid, further supports the likelihood of microbial bioconversion of plastic into simpler bioactive compounds (Mohanan et al. 2020). Collectively, the metabolite profile observed here highlights the potential of this bioconversion system as a bio-based strategy for environmentally friendly plastic waste degradation.

Figure 7.A presents a heatmap illustrating the temporal dynamics of key intermediate concentrations involved in xenobiotic degradation over a 28-day incubation period. Propylene glycol and glycerol exhibited pronounced increases between days 24 and 28, suggesting their accumulation during the late stages of degradation. Benzyl alcohol, prominently detected on day 20, is recognized as a central intermediate in the toluene degradation pathway. Palmitic and stearic acids were consistently detected across most time points, except on day 12, indicating their potential role as lipid-derived by-products. In contrast, compounds such as ethylene glycol butyl ether (notably present on days 4, 8, and 12) and 2,4-di-tert-butylphenoxytrimethylsilane (detected broadly except on day 16) likely reflect early-phase interaction or initial breakdown processes. The observed variation in compound intensity and emergence timing emphasizes the necessity for pathway-specific validation and flux-based quantification to clarify intermediary functions and enzymatic contributions.

The GC-MS analysis also reported numerous organic compounds crucial to different metabolic pathways (Figure 7.A). Myristic acid, essential for lipopolysaccharide synthesis, and glycerol, associated with glycerolipid metabolism, were also identified, and with benzyl alcohol, a by-product of toluene degradation.

The results of the PCA for intermediate compounds are presented in Figure 7.B. The PCA biplot (PC1: 35.77%, PC2: 24.48%) explains 60.25% of the total variance, indicating moderate but meaningful separation in metabolite profiles during the time course of polystyrene (styrofoam) degradation. Early-phase samples (days 0-4) cluster in the upper right, strongly associated with compounds such as ethylene glycol butyl ether and 2-hydroxybutyric acid.

These suggest early oxidative and hydrolytic reactions, often linked to the initial breakdown of polystyrene chains and microbial metabolism of monoaromatic byproducts (Zhang et al. 2022).

As degradation progresses (days 12-20), samples begin toward the lower central quadrant, associated with alcohols (benzyl alcohol), amines (ethanamine), and plasticizer-derived compounds such as bisphenol A monomethyl ether and phthalates, which are commonly released during polystyrene depolymerization or additive leaching. The presence of trimethylsilyl carbamate and monopalmitin may indicate lipid synthesis or stress response pathways during mid-phase degradation (Zhang et al. 2022). Late-phase samples (days 24-28) are located in the lower right quadrant, closely associated with propylene glycol, silanol derivatives, and N, N′-bis(trimethylsilyl)trifluoroacetamidine. These suggest advanced metabolic transformation, possibly indicating microbial assimilation of simpler carbon fragments or secondary metabolites formed from polystyrene decomposition (Cai et al. 2023). The detection of degradation byproducts and surfactant-like compounds in this phase supports active microbial degradation and adaptation.

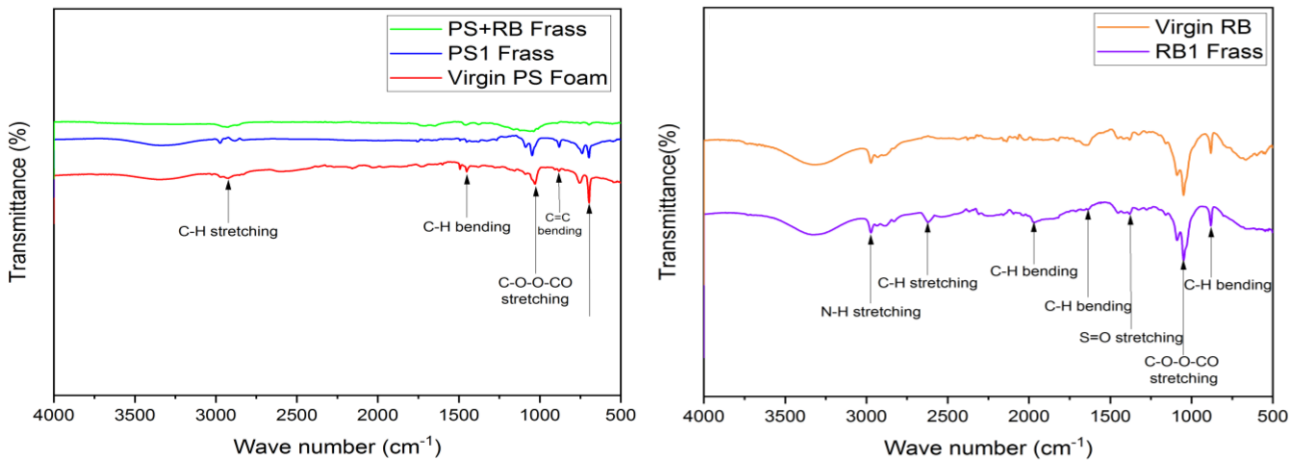

A **B**

Figure 5. FTIR spectrum analysis of frass samples from different mealworm diets. A. Comparison of frass samples from PS1 and PS+RB diets with virgin PS foam, B. Comparison of frass from the RB1 diet with virgin rice bran

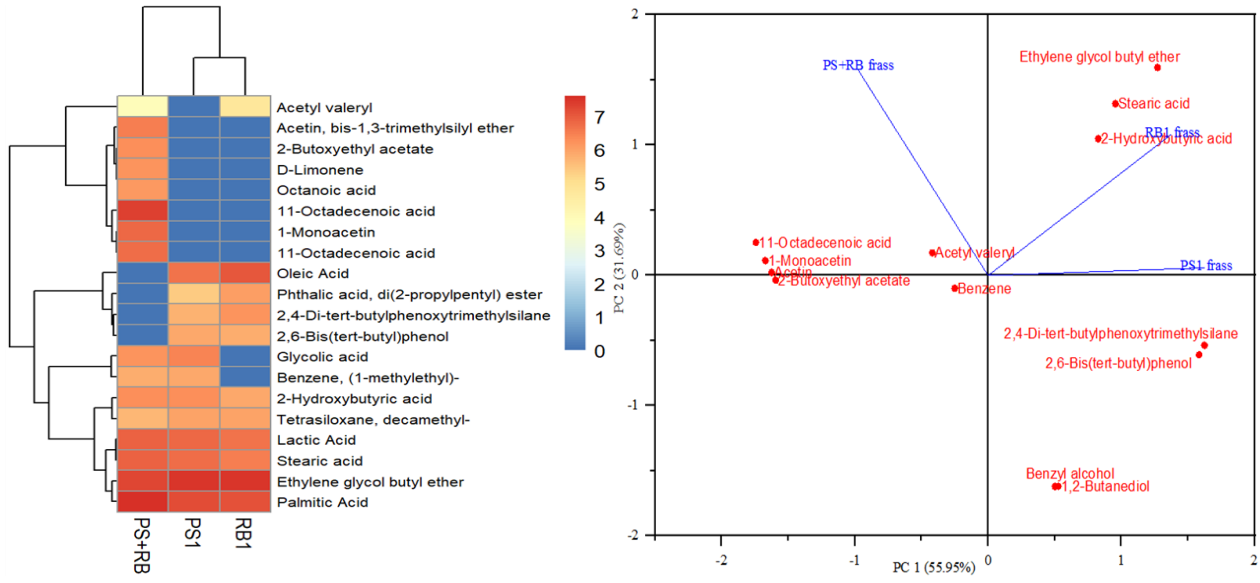

A **B**

Figure 6. A. Heatmap of the top 20 most abundant chemical compounds identified in the frass. The heatmap displays compound abundance levels using a color gradient, where blue indicates low relative abundance and red denotes high relative abundance. The color scale bar ranges from 0 to 7, representing log-transformed intensity values derived from GC-MS analysis. Compounds are listed on the vertical axis, while sample groups are aligned along the horizontal axis, B. Principal Component Analysis (PCA) of mealworm frass samples. The figure shows a PCA biplot illustrating the relationship between various chemical compounds (represented by red dots) and sample treatments (represented by blue vectors) in the mealworm frass. Heatmap and PCA Analysis of Metabolites in Xenobiotic Degradation

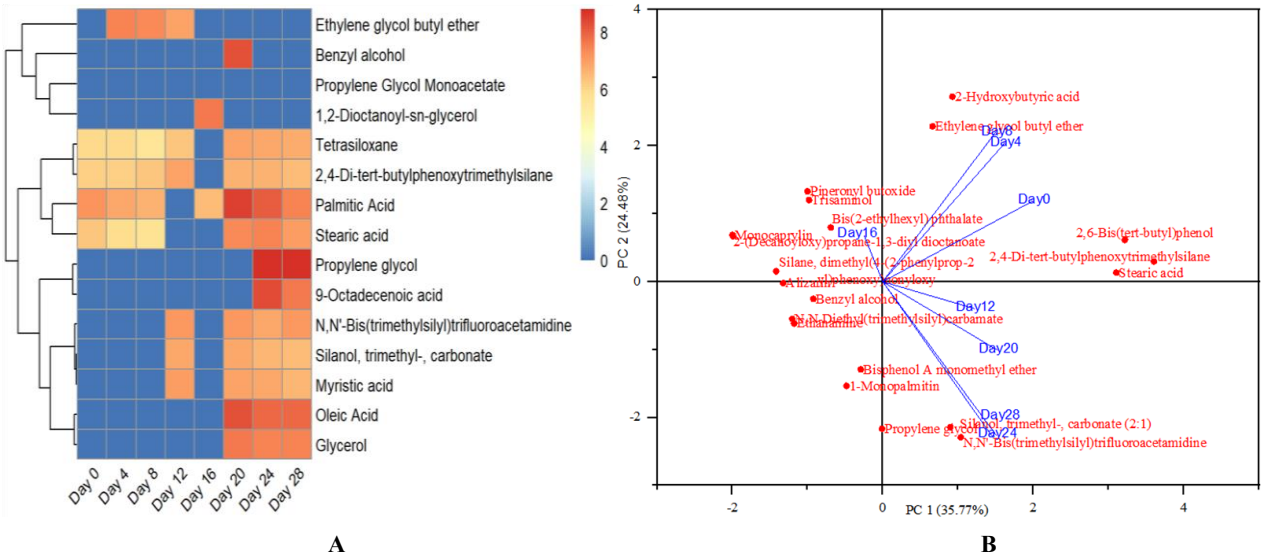

A B

Figure 7. A. Heatmap of the top 20 most abundant major xenobiotic degradation intermediates identified in the Bushnell Haas media. The heatmap displays compound abundance levels using a color gradient, where blue indicates low relative abundance and red denotes high relative abundance. The color scale bar ranges from 0 to 8, representing log-transformed intensity values derived from GC-MS analysis. Compounds are listed on the vertical axis, while time (days) is aligned along the horizontal axis, B. PCA results of intermediate compounds detected in the BH liquid medium during a 28 days

Metabolites related to polystyrene degradation

Analysis of mealworm frass via GC-MS revealed the presence of lactic acid as the sole identified compound associated with PS degradation, consistent with its role as a terminal metabolite in the styrene degradation pathway (Figure 3). However, lactic acid was not exclusively detected in mealworms fed PS-containing diets (PS1 and PS+RB groups), also appearing in frass from the rice bran (RB1) diet group (Figure 6), suggesting its non-specificity to PS degradation in this context. This finding contrasts with the study by Quan et al. (2023), which identified six distinct metabolites linked to the PS degradation pathway in *Zophobas atratus*, namely phenylacetic acid, L-2-aminoadipic acid, 5-hydroxy-L-lysine, pyrocatechol, and 2-hydroxyacetophenone, indicating a more comprehensive metabolic breakdown of PS in that species.

GC-MS analysis identified benzyl alcohol as one of the dominant compounds in the BH media extract. Based on a search of the KEGG pathway database, benzyl alcohol is indicated as an intermediate in the toluene degradation pathway (Figure 8). It is known as an important intermediate in the catabolism of aromatic compounds, including toluene. Generally, the biodegradation of toluene involves oxidation to benzyl alcohol, which is subsequently converted to benzaldehyde and benzoic acid.

The GC-MS analysis identified key metabolites, benzyl alcohol and lactic acid, which serve as critical intermediates in PS degradation pathways. Benzyl alcohol, detected in both frass and BH medium, aligns with the toluene degradation pathway (KEGG), suggesting its role as a transitional product during PS breakdown. Its presence, coupled with the enzymatic activity of 3-hydroxyacyl-CoA dehydrogenase (EC 1.1.1.35), supports the hypothesis of a benzylsuccinate-mediated route for aromatic compound metabolism. Meanwhile, lactic acid, though non-specific to PS diets, indicates terminal oxidation in the styrene degradation pathway, consistent with its production via phenylacetaldehyde dehydrogenase (EC 1.2.1.39). The absence of styrene monomers implies rapid conversion to downstream intermediates, while fatty acids (e.g., palmitic and stearic acid) likely reflect microbial lipid metabolism from fragmented PS-derived carbon. These findings collectively underscore the gut microbiome's capacity to funnel PS-derived compounds into central metabolic pathways, albeit with variability influenced by diet and microbial community dynamics. Further isotopic tracing could validate these proposed pathways and quantify flux rates.

Potential metabolic pathways of PS plastics by mealworm gut microbiome

Based on enzymatic data from metabolomic analysis, a proposed metabolic pathway for PS degradation by the mealworm gut microbiome suggests that depolymerized PS is converted to styrene, which then enters the styrene-cis-2,3-dihydrodiol pathway, ultimately yielding lactic acid as the end product (Figure 3). However, shotgun metagenomic data reveal the presence of enzymes such as phenylacetaldehyde dehydrogenase (EC:1.2.1.39), homogentisate 1,2-dioxygenase (EC:1.13.11.5), and fumarylacetoacetase (EC:3.7.1.2). These findings suggest an alternative or parallel pathway where styrene is converted to styrene oxide, eventually leading to fumarate or acetoacetate as terminal compounds (Figure 3). This contrasts with the findings of Quan et al. (2023), whose metabolomic study of *Z. atratus* gut proposed a different pathway where styrene is converted to phenylacetic acid and subsequently to L-2-aminoadipate through a two-step reaction.

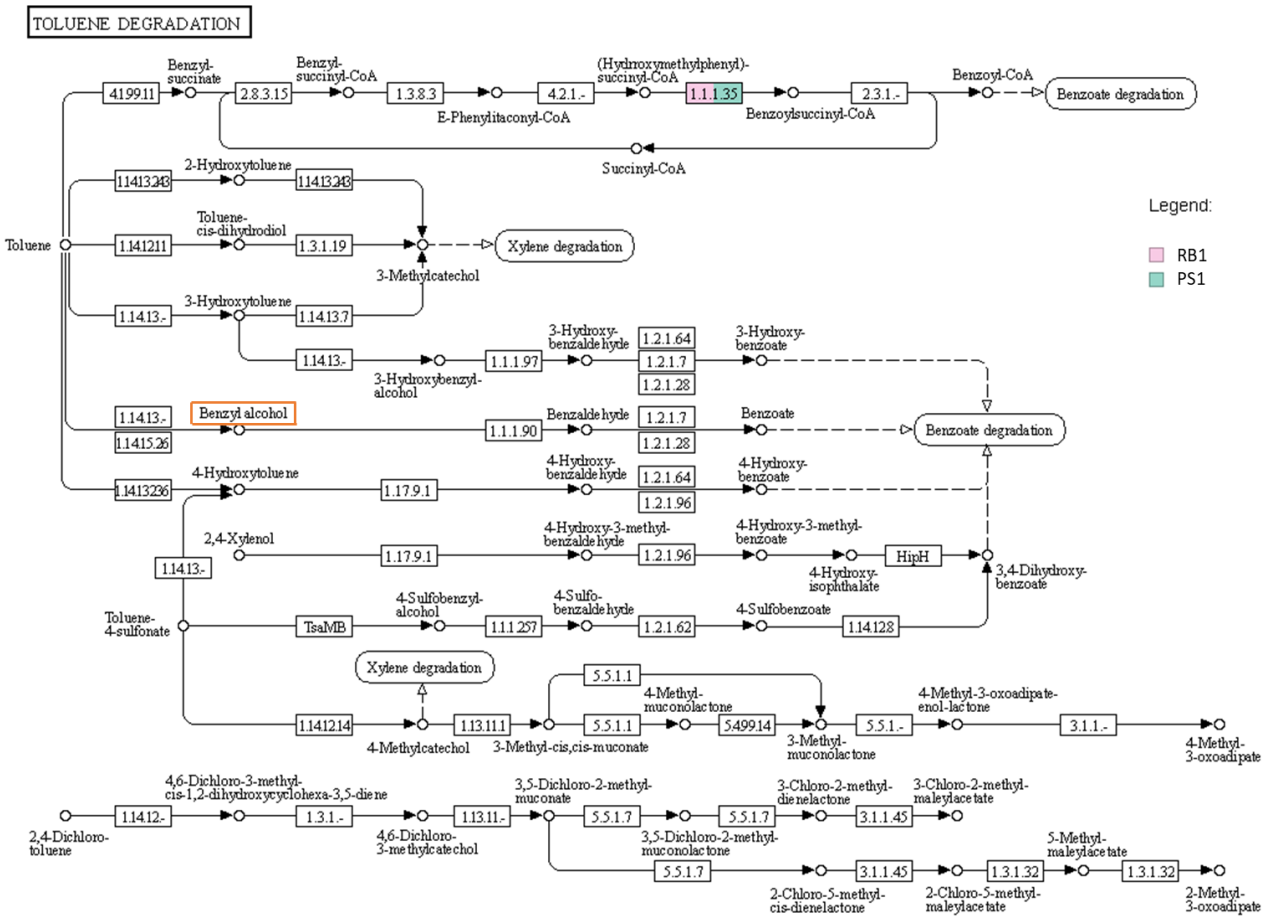

Figure 8. A KEGG pathway visualization produced by the MEGAN software (Huson et al. 2016) showing toluene degradation, highlighting the presence of 3-hydroxyacyl-CoA dehydrogenase (EC 1.1.1.35) detected in the functional genes of gut microbiota from mealworm fed rice bran RB1 and PS1 diets, with benzyl alcohol as an intermediate compound indicated by an orange box

Metagenomic analysis of the gut microbiome community of mealworms diet revealed the presence of a gene encoding 3-hydroxyacyl-CoA dehydrogenase enzyme (EC 1.1.1.35). This enzyme plays a role in the toluene degradation pathway via the benzylsuccinate route, particularly in the conversion of aromatic compounds into benzylsuccinyl coenzyme A (Figure 8). This metabolite can subsequently enter more complex aromatic degradation pathways compounds that can be accessed by the tricarboxylic acid cycle. The identification of benzyl alcohol in the metabolomic analysis, coupled with the detection of 3-hydroxyacyl-CoA dehydrogenase (EC 1.1.1.35) in the metagenomic data, suggests the potential utilization of aromatic compound degradation pathways by the gut microbiome of mealworms for the metabolism of PS fragments.

The schematic of the research results presented in Figure 9 illustrates the PS biodegradation mechanism by mealworm, involving synergistic interplay of physicochemical processes and gut microbiome activity. Initially, PS undergoes mechanical fragmentation by the larval mandibles into smaller particles, increasing the surface area for microbial degradation. Subsequently, the secretion of bioemulsifiers by the larvae enhances the bioavailability of PS fragments, facilitating microbial action in the gut. Metagenomic analysis revealed the dominance of the genus *Nocardioides* in mealworm diets, rice bran, rice bran, and PS. At the same time, At the same time, *Burkholderia* and *Oceanobacter* were specifically associated with PS-fed groups, consistent with their established roles in hydrocarbon degradation pathways. Gut microbial consortium produces potential enzymes, such as monooxygenases and aldehyde dehydrogenases, which participate in xenobiotic degradation pathways (e.g., styrene/toluene pathways). Metabolomic profiling confirmed the presence of intermediates like lactic acid and benzyl alcohol, along with end products including mineralized CO_2, microbial biomass, and frass (a mixture of residual PS fragments and microbes). These findings highlight the host-microbiome synergy in converting PS into metabolizable compounds that support larval energy gain.

The interaction among enzymes, microbial species, and metabolites is visualized in Figure 10. Based on KEGG pathway analysis, several key enzymes involved in styrene degradation were identified in the gut system of *Tenebrio molitor*. These include phenylacetaldehyde dehydrogenase (EC 1.2.1.39), amidase (EC 3.5.1.4), homogentisate 1,2-dioxygenase (EC 1.13.11.5), fumarylacetoacetase (EC 3.7.1.2), and 3-hydroxyacyl-CoA dehydrogenase (EC 1.1.1.35). By comparing KEGG data and the gut microbiome database of mealworms, several bacterial

species that produce these enzymes were found: *Pseudomonas otitidis*, *Chania multitudinisentens*, *Shewanella vesiculosa*, and *Acinetobacter pittii*. The presence of these species supports the idea that the styrene degradation pathway is active in the mealworm digestive system. In addition, metabolomic analysis detected lactate, which is part of the styrene degradation pathway and may reflect downstream fermentative or oxidative activity.

In the toluene degradation pathway, the enzyme 3-hydroxyacyl-CoA dehydrogenase (EC 1.1.1.35) produced by *C. multitudinisentens*, along with the intermediate metabolite benzyl alcohol. This compound is an early oxidation product of toluene and shows microbial reactivity toward toxic aromatic compounds. The interaction among enzymes, microbial species, and metabolites visualized in Figure 10 demonstrates that the gut microbiota of *T. molitor* integrated capabilities for degrading aromatic pollutants. It suggests that this system is not only taxonomically diverse, but also functionally diverse and well-adapted to break down xenobiotic compounds (Engel and Moran 2013).

In the unidentified degradation pathway, this study uncovered several key enzymes that may play a role in the transformation of complex compounds. These enzymes include amidase (EC 3.5.1.4), phenylacetaldehyde dehydrogenase (EC 1.2.1.39), homogentisate 1,2-dioxygenase (EC 1.13.11.5), acyl-CoA synthetase (EC 6.2.1.3), and carboxylesterase (EC 3.1.1.3), all reported by Mamtimin et al. (2023). These findings suggest the existence of alternative degradation routes for long-chain fatty compounds that have not been fully mapped in conventional metabolic databases.

Taxonomic analysis further revealed the presence of microbial genera, including *Burkholderia*, *Pseudomonas*, and *Spiroplasma*, which are known to be associated with enzyme expression. *Burkholderia* is particularly recognized for its ecological versatility and role in the biodegradation of aromatic and lipid compounds (Hou and Majumder 2021). *Pseudomonas* and *Spiroplasma* were also identified in recent functional microbiome studies (Mamtimin et al. 2023). These genera are known for their metabolic plasticity, enabling them to adapt to diverse ecological conditions and contribute actively to microbial community dynamics.

From metabolomic perspective, the detection of long-chain fatty acids such as palmitic acid, oleic acid, stearic acid, and myristic acid supports the hypothesis that these microbes can oxidize and metabolize lipid-derived substrates. These metabolic activities likely contribute to microbial energy cycling and carbon turnover in the gut ecosystem (Sousa et al. 2007). Overall, these results emphasize the importance of exploring undefined metabolic pathways to understand microbial ecology and functional biodiversity better. The identification of key enzymes, microbial taxa, and associated metabolites highlights the adaptive capacity of gut microbiota to process complex organic compounds and maintain environmental balance. This opens opportunities for harnessing insect microbiomes in biotechnological applications such as lipid waste conversion and bioremediation (Compant et al. 2008; Udaondo et al. 2024).

SEM analysis of PS degradation by mealworm gut microbes

The findings of this study revealed the significant potential of gut microbes in degrading PS plastic. PS biodegradation was observed by analyzing surface images of PS films incubated with mealworm gut extracts in BH liquid medium. SEM was utilized to visualize surface changes (Figure 11). At 5000× magnification, the control PS film exhibited a smooth surface (Figure 11.A). After 28 days of incubation with gut microbes, SEM images showed numerous bacteria of various morphologies attached to the PS film surface (Figure 11.B), highlighting the strong potential of gut microbes in degrading PS plastic (Quan et al. 2023). After rinsing the PS film with SDS, SEM analysis revealed significant alterations, including holes, cavities, and increased surface roughness (Figure 11.C). These changes not only provide attachment sites for microorganisms but also offer protection from shear pressures in liquid environments, which contributes to film degradation by bacteria (Lin et al. 2024). Changes on the plastic surface are the hallmark of plastic degradation by microorganisms, primarily driven by enzymatic activity (Di Liberto et al. 2024).

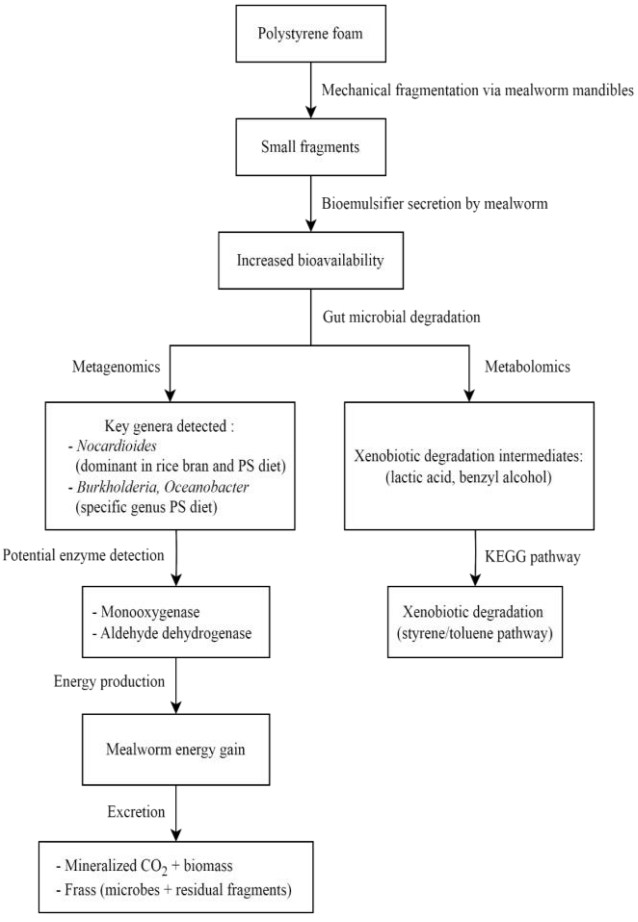

Figure 9. Schematic representation of the PS biodegradation in the mealworm gut, illustrating potential enzymes involved in PS degradation, key gut microbiome genera associated with xenobiotic metabolism, intermediate degradation compounds, and the interplay between microbial activity and host digestive processes

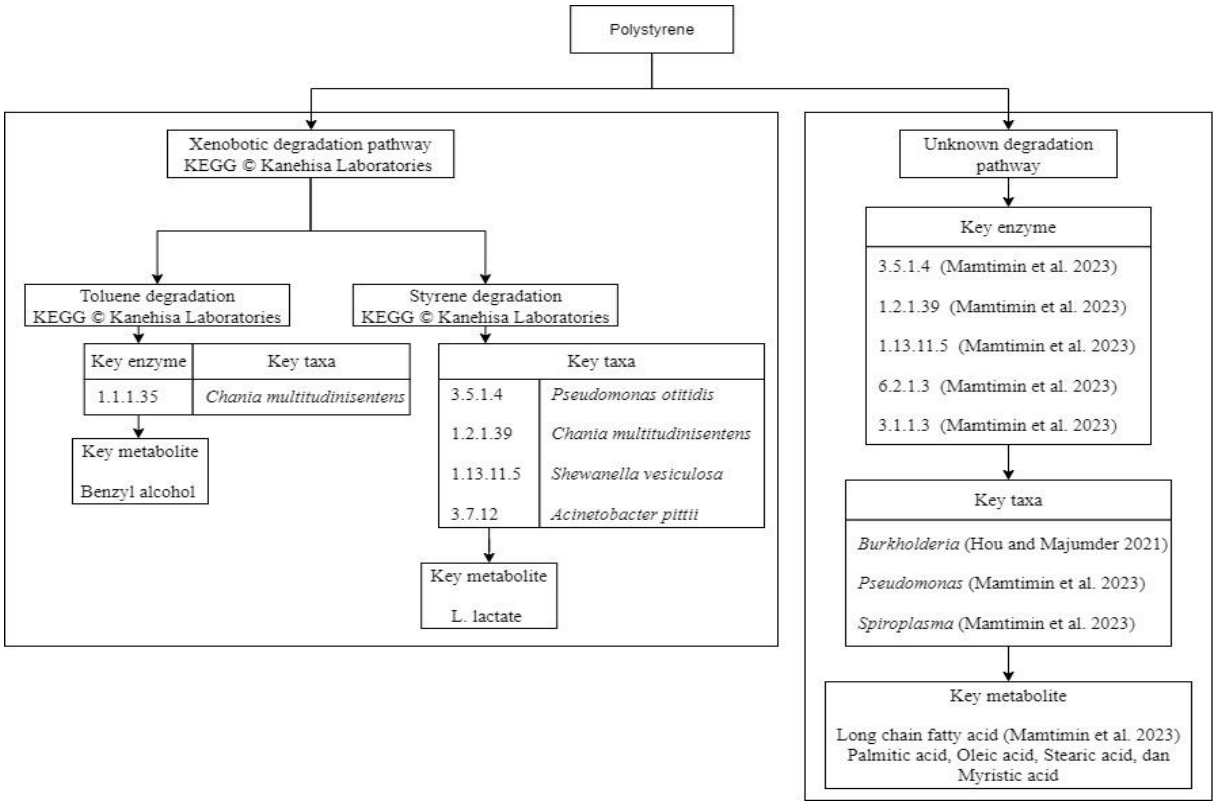

Figure 10. Summarizing interacting microbial taxa-metabolite-enzyme

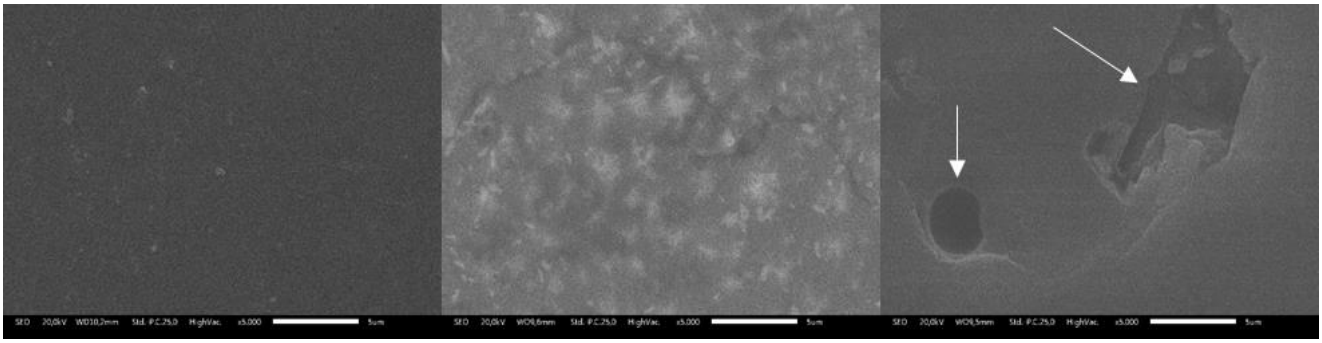

A **B** **C**

Figure 11. Scanning Electron Microscope (SEM) of PS film after 28 days. A. PS film without treatment (control), B. PS film without SDS treatment, C. PS film with SDS treatment, the white arrows indicate notable surface alterations, including pore formation and structural disintegration

This study underscores the dual ecological and biotechnological significance of mealworms and their gut microbiome in tackling polystyrene (PS) pollution. Firstly, it demonstrates the mealworms' impressive biodegradation capacity—evidenced by a 6.38% PS mass reduction in vivo and 3.49% in vitro—supported by surface erosion observed via SEM and chemical transformation confirmed by FTIR. The detection of key degradation by-products such as lactic acid and benzyl alcohol, along with potential enzymes including monooxygenases and cytochrome P450, suggests active metabolic pathways PS breakdown. Secondly, this research reveals the complex adaptability and functional diversity of the mealworm gut microbiome. Taxonomic analysis showed Proteobacteria as the dominant phylum, with enrichment of hydrocarbon-degrading genera such as *Burkholderia*, *Oceanobacter*, and *Nocardioides* under PS feeding conditions. Functional metagenomics revealed that microbial communities play a significant role in xenobiotic degradation through styrene and toluene pathways. The identification of rare, low-abundance taxa performing specialized degradation functions indicates that gut microbial biodiversity harbors untapped enzymatic potential. Ecologically, these findings the role of insect-microbe as natural biodegraders that can contribute to the resilience of

terrestrial ecosystems increasingly burdened by anthropogenic pollutants. The ability of mealworms and their gut consortia to metabolize synthetic polymers suggests a previously underappreciated ecological service—one that may influence microplastic turnover in soil food webs and affect trophic transfer dynamics. Preserving these symbiotic communities is crucial not only for sustaining host health and ecological resilience but also as a source of future biotechnological tools. As anthropogenic pressures and plastic pollution accelerate, safeguarding these microbial reservoirs could pave the way for sustainable biocatalyst development and ecosystem-based waste remediation strategies.

ACKNOWLEDGEMENTS

This research is funded by The Osaka Gas Foundation of International Cultural Exchange (OGFICE) Research Grant for Fiscal Year 2021/2022 and the IPR ITB Research Grant 2025. The authors express their gratitude to colleagues at the Institute of Technology Bandung and the National Research and Innovation Agency (BRIN) in Bandung and Serpong, Indonesia, for their support in providing access to analytical Servers, SEM, GC-MS, and FTIR through ELSA BRIN. We also acknowledge PT. Tekad Mandiri Citra for their cooperation in assisting the research and PhD studies through the provision of facilities, financial assistance, and chemicals.

REFERENCES

Andrews S. 2010. FastQC: A quality control tool for high throughput sequence data. www.bioinformatics.babraham.ac.uk/projects/fastqc.

Atanasova N, Stoitsova S, Paunova-Krasteva T, Kambourova M. 2021. Plastic degradation by extremophilic bacteria. Intl J Mol Sci 22 (11): 5610. DOI: 10.3390/ijms22115610.

Bai X, Huang Z, Duraj-Thatte AM, Ebert MP, Zhang F, Burgermeister E, Liu X, Scott BM, Li G, Zuo T. 2023. Engineering the gut microbiome. Nat Rev Bioeng 1: 665-679. DOI: 10.1038/s44222-023-00072-2.

Bilal H, Raza H, Bibi H, Bibi T. 2021. Plastic biodegradation through insects and their symbionts microbes: A review. J Bioresour Manag 8 (4): 95-103. DOI: 10.35691/jbm.1202.0206.

Brandon AM, Gao S-H, Tian R, Ning D, Yang S-S, Zhou J, Wu W-M, Criddle CS. 2018. Biodegradation of polyethylene and plastic mixtures in mealworms (larvae of *Tenebrio molitor*) and effects on the gut microbiome. Environ Sci Technol 52 (11): 6526-6533. DOI: 10.1021/acs.est.8b02301.

Brzeszcz J, Steliga T, Ryszka P, Kaszycki P, Kapusta P. 2024. Bacteria degrading both n-alkanes and aromatic hydrocarbons are prevalent in soils. Environ Sci Pollut Res Intl 31 (4): 5668-5683. DOI: 10.1007/s11356-023-31405-8.

Buchfink B, Xie C, Huson DH. 2014. Fast and sensitive protein alignment using DIAMOND. Nat Methods 12: 59-60. DOI: 10.1038/nmeth.3176.

Cai Z, Li M, Zhu Z, Wang X, Huang Y, Li T, Gong H, Yan M. 2023. Biological degradation of plastics and microplastics: A recent perspective on associated mechanisms and influencing factors. Microorganisms 11: 1661. DOI: 10.3390/microorganisms11071661.

Calmont B, Soldati F. 2008. Ecologie et biologie de *Tenebrio opacus* Duftschmid, 1812 Distribution et détermination des espèces françaises du genre *Tenebrio* Linnaeus, 1758. R.A.R.E XVII (3): 81-87.

Castro AR, Martins G, Salvador AF, Cavaleiro AJ. 2022. Iron compounds in anaerobic degradation of petroleum hydrocarbons: A review. Microorganisms 10: 2142. DOI: 10.3390/microorganisms10112142.

Chang H, Gu C, Wang M, Chang Z, Zhou J, Yue M, Chen J, Qin X, Feng Z. 2024. Integrating shotgun metagenomics and metabolomics to elucidate the dynamics of microbial communities and metabolites in fine flavor cocoa fermentation in Hainan. Food Res Intl 177: 113849. DOI: 10.1016/j.foodres.2023.113849.

Compant S, Nowak J, Coenye T, Clément C, Barka EA. 2008. Diversity and occurrence of *Burkholderia* spp. in the natural environment. FEMS Microbiol Rev 32 (4): 607-626. DOI: 10.1111/j.1574-6976.2008.00113.x.

Dar MA, Xie R, Zabed HM, Pawar KD, Dhole NP, Sun J. 2024. Current paradigms and future challenges in harnessing gut bacterial symbionts of insects for biodegradation of plastic wastes. Insect Sci 32 (3): 726-752. DOI: 10.1111/1744-7917.13417.

De Filippis F, Bonelli M, Bruno D et al. 2023. Plastics shape the black soldier fly larvae gut microbiome and select for biodegrading functions. Microbiome 11 (1): 205. DOI: 10.1186/s40168-023-01649-0.

Di Liberto EA, Battaglia G, Pellerito R, Curcuruto G, Dintcheva NT. 2024. Biodegradation of polystyrene by plastic-eating Tenebrionidae larvae. Polymers 16 (10): 1404. DOI: 10.3390/polym16101404.

dos Santos IB, Pereira APdA, de Souza AJ, Cardoso EJBN, da Silva FG, Oliveira JTC, Verdi MCQ, Sobral JK. 2022. Selection and characterization of *Burkholderia* spp. for their plant-growth promoting effects and influence on maize seed germination. Front Soil Sci 1: 805094. DOI: 10.3389/fsoil.2021.805094.

Engel P, Moran NA. 2013. The gut microbiota of insects - diversity in structure and function. FEMS Microbiol Rev 37 (5): 699-735. DOI: 10.1111/1574-6976.12025.

Fan Y, Wang D, Yang JX, Ning D, He Z, Zhang P, Rocha AM, Xiao N, Michael JP, Walker KF, Joyner DC, Pan C, Adams MWW, Fields MW, Alm EJ, Stahl DA, Hazen TC, Adams PD, Arkin AP, Zhou J. 2025. Modest functional diversity decline and pronounced composition shifts of microbial communities in a mixed waste-contaminated aquifer. Microbiome 13 (1): 106. DOI: 10.1186/s40168-025-02105-x.

Fortunato CS, Larson B, Butterfield DA, Huber JA. 2018. Spatially distinct, temporally stable microbial populations mediate biogeochemical cycling at and below the seafloor in hydrothermal vent fluids. Environ Microbiol 20 (2): 769-784. DOI: 10.1111/1462-2920.14011.

Gautam A, Felderhoff H, Bagci C, Huson DH. 2022. Using AnnoTree to get more assignments, faster, in DIAMOND+MEGAN microbiome analysis. mSystems 7 (1): e0140821. DOI: 10.1128/msystems.01408-21.

Haider K, Abbas D, Galian J, Ghafar MA, Kabir K, Ijaz M, Hussain M, Khan KA, Ghramh HA, Raza A. 2025. The multifaceted roles of gut microbiota in insect physiology, metabolism, and environmental adaptation: Implications for pest management strategies. World J Microbiol Biotechnol 41 (3): 75. DOI: 10.1007/s11274-025-04288-9.

Hahladakis JN, Velis CA, Weber R, Iacovidou E, Purnell P. 2018. An overview of chemical additives present in plastics: Migration, release, fate and environmental impact during their use, disposal and recycling. J Hazard Mater 344: 179-199. DOI: 10.1016/j.jhazmat.2017.10.014.

He L, Yang S-S, Ding J, Chen C-X, Yang F, He Z-L, Pang J-W, Peng B-Y, Zhang Y, Xing D-F, Ren N-Q, Wu W-M. 2024. Biodegradation of polyethylene terephthalate by *Tenebrio molitor*: Insights for polymer chain size, gut metabolome and host genes. J Hazard Mater 465: 133446. DOI: 10.1016/j.jhazmat.2024.133446.

Hou L, Majumder EL-W. 2021. Potential for and distribution of enzymatic biodegradation of polystyrene by environmental microorganisms. Materials 14 (3): 503. DOI: 10.3390/ma14030503.

Ho BT, Roberts TK, Lucas S. 2018. An overview on biodegradation of polystyrene and modified polystyrene: The microbial approach. Crit Rev Biotechnol 38: 308-320. DOI: 10.1080/07388551.2017.1355293.

Huson DH, Beier S, Flade I, Górska A, El-Hadidi M, Mitra S, Ruscheweyh H-J, Tappu R. 2016. MEGAN community edition - interactive exploration and analysis of large-scale microbiome sequencing data. PLoS Comput Biol 12: e1004957. DOI: 10.1371/journal.pcbi.1004957.

Kaltenpoth M, Flórez LV, Vigneron A, Dirksen P, Engl T. 2025. Origin and function of beneficial bacterial symbioses in insects. Nat Rev Microbiol 23 (9): 551-567. DOI: 10.1038/s41579-025-01164-z.

Kundungal H, Gangarapu M, Sarangapani S, Patchaiyappan A, Devipriya SP. 2019. Efficient biodegradation of polyethylene (HDPE) waste by the plastic-eating lesser waxworm (*Achroia grisella*). Environ Sci Pollut Res Intl 26: 18509-18519. DOI: 10.1007/s11356-019-05038-9.

Kundungal H, Synshiang K, Devipriya SP. 2021. Biodegradation of polystyrene wastes by a newly reported honey bee pest *Uloma* sp. larvae: An insight to the ability of polystyrene-fed larvae to complete its life cycle. Environ Chall 4: 100083. DOI: 10.1016/j.envc.2021.100083.

Ladino-Orjuela G, Gomes E, da Silva R, Salt C, Parsons JR. 2016. Metabolic pathways for degradation of aromatic hydrocarbons by bacteria. Rev

Environ Contam Toxicol 237: 105-121. DOI: 10.1007/978-3-319-23573-8_5.
Lepcha A, Kumar R, Dindhoria K, Bhargava B, Pati AM, Kumar R. 2025. Metagenomic insights into the functional potential of non-sanitary landfill microbiomes in the Indian Himalayan region, highlighting key plastic degrading genes. J Hazard Mater 484: 136642. DOI: 10.1016/j.jhazmat.2024.136642.
Li D, Liu C-M, Luo R, Sadakane K, Lam T-W. 2015. MEGAHIT: An ultra-fast single-node solution for large and complex metagenomics assembly via succinct de Bruijn graph. Bioinformatics 31 (10): 1674-1676. DOI: 10.1093/bioinformatics/btv033.
Lienkamp AC, Burnik J, Heine T, Hofmann E, Tischler D. 2021. Characterization of the glutathione s-transferases involved in styrene degradation in *Gordonia rubripertincta* CWB2. Microbiol Spectr 9 (1): e0047421. DOI: 10.1128/spectrum.00474-21.
Lin W, Yao Y, Su T, Wang Z. 2024. Biodegradation of polystyrene by bacteria isolated from the yellow mealworm (*Tenebrio Molitor*) gut. J Environ Chem Eng 12 (2): 112071. DOI: 10.1016/j.jece.2024.112071.
López-Hernández MG, Rincón-Rosales R, Rincón-Molina CI, Manzano-Gómez LA, Gen-Jiménez A, Maldonado-Gómez JC, Rincón-Molina FA. 2025. Diversity and functional potential of gut bacteria associated with the insect *Arsenura armida* (Lepidoptera: Saturniidae). Insects 16 (7): 711. DOI: 10.3390/insects16070711.
Lou Y, Ekaterina P, Yang SS, Lu B, Liu B, Ren N, Corvini PFX, Xing D. 2020. Biodegradation of polyethylene and polystyrene by greater wax moth larvae (*Galleria mellonella* L.) and the effect of co-diet supplementation on the core gut microbiome. Environ Sci Technol 54: 2821-2831. DOI: 10.1021/acs.est.9b07044.
Lou Y, Li Y, Lu B, Liu Q, Yang S-S, Liu B, Ren N, Wu W-M, Xing D. 2021. Response of the yellow mealworm (*Tenebrio molitor*) gut microbiome to diet shifts during polystyrene and polyethylene biodegradation. J Hazard Mater 416: 126222. DOI: 10.1016/j.jhazmat.2021.126222.
Lozupone CA, Stombaugh JI, Gordon JI, Jansson JK, Knight R. 2012. Diversity, stability and resilience of the human gut microbiota. Nature 489 (7415): 220-230. DOI: 10.1038/nature11550.
Ma Y, Wang J, Liu Y, Wang X, Zhang B, Zhang W, Chen T, Liu G, Xue L, Cui X. 2023. Nocardioides: "Specialists" for hard-to-degrade pollutants in the environment. Molecules 28: 7433. DOI: 10.3390/molecules28217433.
Mamtimin T, Han H, Khan A, Feng P, Zhang Q, Ma X, Fang Y, Liu P, Kulshrestha S, Shigaki T, Li X. 2023. Gut microbiome of mealworms (*Tenebrio molitor* larvae) show similar responses to polystyrene and corn straw diets. Microbiome 11 (1): 98. DOI: 10.1186/s40168-023-01550-w.
Mannaa M, Park I, Seo YS. 2018. Genomic features and insights into the taxonomy, virulence, and benevolence of plant-associated *Burkholderia* species. Intl J Mol Sci 20: 121. DOI: 10.3390/ijms20010121.
Maron P-A, Sarr A, Kaisermann A, Lévêque J, Mathieu O, Guigue J, Karimi B, Bernard L, Dequiedt S, Terrat S, Chabbi A, Ranjard L. 2018. High microbial diversity promotes soil ecosystem functioning. Appl Environ Microbiol 84: e02738-17. DOI: 10.1128/aem.02738-17.
Mesnage R, Antoniou MN, Tsoukalas D, Goulielmos GN, Tsatsakis A. 2018. Gut microbiome metagenomics to understand how xenobiotics impact human health. Curr Opin Toxicol 11-12: 51-58. DOI: 10.1016/j.cotox.2019.02.002.
Miglani R, Parveen N, Kumar A, Ansari MA, Khanna S, Rawat G, Panda AK, Bisht SS, Upadhyay J, Ansari MN. 2022. Degradation of xenobiotic pollutants: An environmentally sustainable approach. Metabolites 12 (9): 818. DOI: 10.3390/metabo12090818.
Mikaelyan A, Dietrich C, Köhler T, Poulsen M, Sillam-Dussès D, Brune A. 2015. Diet is the primary determinant of bacterial community structure in the guts of higher termites. Mol Ecol 24 (20): 5284-5295. DOI: 10.1111/mec.13376.
Mishra S, Lin Z, Pang S, Zhang W, Bhatt P, Chen S. 2021. Recent advanced technologies for the characterization of xenobiotic-degrading microorganisms and microbial communities. Front Bioeng Biotechnol 9: 632059. DOI: 10.3389/fbioe.2021.632059.
Mitzscherling J, MacLean J, Lipus D, Bartholomäus A, Mangelsdorf K, Lipski A, Roddatis V, Liebner S, Wagner D. 2022. *Nocardioides alcanivorans* sp. nov., a novel hexadecane-degrading species isolated from plastic waste. Intl J Syst Evol Microbiol 72 (4): 1-11. DOI: 10.1099/ijsem.0.005319.
Mohanan N, Montazer Z, Sharma PK, Levin DB. 2020. Microbial and enzymatic degradation of synthetic plastics. Front Microbiol 11: 580709. DOI: 10.3389/fmicb.2020.580709.
Mohapatra B, Phale PS. 2021. Microbial degradation of naphthalene and substituted naphthalenes: Metabolic diversity and genomic insight for bioremediation. Front Bioeng Biotechnol 9: 602445. DOI: 10.3389/fbioe.2021.602445.
Mondal S, Somani J, Roy S, Babu A, Pandey AK. 2023. Insect microbial symbionts: Ecology, interactions, and biological significance. Microorganisms 11: 2665. DOI: 10.3390/microorganisms11112665.
Muñoz-Benavent M, Pérez-Cobas AE, García-Ferris C, Moya A, Latorre A. 2021. Insects' potential: Understanding the functional role of their gut microbiome. J Pharm Biomed Anal 194: 113787. DOI: 10.1016/j.jpba.2020.113787.
Olowomofe TO, Oluyege JO, Aderiye BI, Oluwole OA. 2019. Research article degradation of poly aromatic fractions of crude oil and detection of catabolic genes in hydrocarbon-degrading bacteria isolated from Agbabu bitumen sediments in Ondo State. AIMS Microbiol 5 (4): 308-323. DOI: 10.3934/microbiol.2019.4.308.
Pathak VM, Navneet. 2017. Review on the current status of polymer degradation: A microbial approach. Bioresour Bioprocess 4: 15. DOI: 10.1186/s40643-017-0145-9.
Peng B-Y, Chen Z, Chen J, Yu H, Zhou X, Criddle CS, Wu W-M, Zhang Y. 2020. Biodegradation of Polyvinyl Chloride (PVC) in *Tenebrio molitor* (Coleoptera: Tenebrionidae) larvae. Environ Intl 145: 106106. DOI: 10.1016/j.envint.2020.106106.
Pham TQ, Longing S, Siebecker MG. 2023. Consumption and degradation of different consumer plastics by mealworms (*Tenebrio molitor*): Effects of plastic type, time, and mealworm origin. J Clean Prod 403: 136842. DOI: 10.1016/j.jclepro.2023.136842.
Pivato AF, Miranda GM, Prichula J, Lima JEA, Ligabue RA, Seixas A, Trentin DS. 2022. Hydrocarbon-based plastics: Progress and perspectives on consumption and biodegradation by insect larvae. Chemosphere 293: 133600. DOI: 10.1016/j.chemosphere.2022.133600.
Purohit J, Chattopadhyay A, Teli B. 2020. Metagenomic exploration of plastic degrading microbes for biotechnological application. Curr Genomics 21: 253-270. DOI: 10.2174/1389202921999200525155711.
Quan Z, Zhao Z, Liu Z, Wang W, Yao S, Liu H, Lin X, Li QX, Yan H, Liu X. 2023. Biodegradation of polystyrene microplastics by superworms (larve of *Zophobas atratus*): Gut microbiota transition, and putative metabolic ways. Chemosphere 343: 140246. DOI: 10.1016/j.chemosphere.2023.140246.
Quince C, Walker AW, Simpson JT, Loman NJ, Segata N. 2017. Shotgun metagenomics, from sampling to analysis. Nat Biotechnol 35 (9): 833-844. DOI: 10.1038/nbt.3935.
Ramond J-B, Galand PE, Logares R. 2025. Microbioal functional diversity and redundancy: Moving forward. FEMS Microbiol Rev 49: fuae031. DOI: 10.1093/femsre/fuae031.
Ridley Jr RS, Conrad RE, Lindner BG, Woo S, Konstantinidis KT. 2024. Potential routes of plastics biotransformation involving novel plastizymes revealed by global multi-omic analysis of plastic associated microbes. Sci Rep 14: 8798. DOI: 10.1038/s41598-024-59279-x.
Robinson WH. 2005. Urban Insects and Arachnids. A Handbook of Urban Entomology. Cambridge University Press, Cambridge. DOI: 10.1017/CBO9780511542718.
Rosado MJ, Rencoret J, Marques G, Gutiérrez A, del Río JC. 2021. Structural characteristics of the guaiacyl-rich lignins from rice (*Oryza sativa* L.) husks and straw. Front Plant Sci 12: 640475. DOI: 10.3389/fpls.2021.640475.
Roswell M, Dushoff J, Winfree R. 2021. A conceptual guide to measuring species diversity. Oikos 130 (3): 321-338. DOI: 10.1111/oik.07202.
Sanders JG, Powell S, Kronauer DJC, Vasconcelos HL, Frederickson ME, Pierce NE. 2014. Stability and phylogenetic correlation in gut microbiota: Lessons from ants and apes. Mol Ecol 23 (6): 1268-1283. DOI: 10.1111/mec.12611.
Sharma AK, Dubey VS. 2021. Metagenome assembly for gut microbial functional diversity associated with xenobiotic degradation. In: De Mandal S, Panda AK, Kumar NS, Bisht SS, Jin F (eds). Metagenomics and Microbial Ecology: Techniques and Applications. CRC Press, Boca Raton.
Son Y-J, Choi SY, Hwang I-K, Nho CW, Kim SH. 2020. Could defatted mealworm (*Tenebrio molitor*) and mealworm oil be used as food ingredients? Foods 9 (1): 40. DOI: 10.3390/foods9010040.
Sousa DZ, Pereia MA, Stams AJM, Alves MM, Smidt H. 2007. Microbial communities involved in anaerobic degradation of long-chain fatty acids. Appl Environ Microbiol 73: 1054-1064. DOI: 10.1128/aem.01723-06.
Srikandace Y, Kamarisima, Putri SP, Aditiawati P. 2025. Optimization of medium components for enhancing antibacterial activity of marine

Streptomyces aureofaciens A3 through response surface methodology. Trends Sci 22 (3): 9144. DOI: 10.48048/tis.2025.9144.

Sun S, Zhang Z, Yu C, Liu Y, Xiao X, Zhao Y. 2021. Complete genome sequence of *Tsuneonella f lava* SS-21NJ, a potential oil sludge bioremediation agent. Microbiol Resour Announc 10 (20): e00216-21. DOI: 10.1128/mra.00216-21.

Teramoto M, Suzuki M, Okazaki F, Hatmanti A, Harayama S. 2009. Oceanobacter-related bacteria are important for the degradation of petroleum aliphatic hydrocarbons in the tropical marine environment. Microbiology 155 (10): 3362-3370. DOI: 10.1099/mic.0.030411-0.

Terova G, Gini E, Gasco L, Moroni F, Antonini M, Rimoldi S. 2021. Effects of full replacement of dietary fishmeal with insect meal from *Tenebrio molitor* on rainbow trout gut and skin microbiota. J Anim Sci Biotechnol 12 (1): 30. DOI: 10.1186/s40104-021-00551-9.

Tsochatzis E, Lopes JA, Gika H, Theodoridis G. 2021a. Polystyrene biodegradation by *Tenebrio molitor* larvae: Identification of generated substances using a GC-MS untargeted screening method. Polymers 13 (1): 17. DOI: 10.3390/polym13010017.

Tsochatzis ED, Berggreen IE, Nørgaard JV, Theodoridis G, Dalsgaard TK. 2021b. Biodegradation of expanded polystyrene by mealworm larvae under different feeding strategies evaluated by metabolic profiling using GC-TOF-MS. Chemosphere 281: 130840. DOI: 10.1016/j.chemosphere.2021.130840.

Udaondo Z, Ramos JL, Abram K. 2024. Unraveling the genomic diversity of the *Pseudomonas putida* group. FEMS Microbiol Rev 48 (6): fuae025. DOI: 10.1093/femsre/fuae025.

Urbanek AK, Rybak J, Hanus-Lorenz B, Komisarczyk DA, Mirończuk AM. 2024. *Zophobas morio* versus *Tenebrio molitor*: Diversity in gut microbiota of larvae fed with polymers. Sci Total Environ 952: 176005. DOI: 10.1016/j.scitotenv.2024.176005.

Urbanek AK, Rybak J, Wróbel M, Leluk K, Mirończuk AM. 2020. A comprehensive assessment of microbiome diversity in *Tenebrio molitor* fed with polystyrene waste. Environ Pollut 262: 114281. DOI: 10.1016/j.envpol.2020.114281.

Vasiliou V, Pappa A, Petersen DR. 2000. Role of aldehyde dehydrogenases in endogenous and xenobiotic metabolism. Chem Biol Interact 129 (1-2): 1-19. DOI: 10.1016/S0009-2797(00)00211-8.

Venegas S, Alarcón C, Araya J, Gatica M, Morin V, Tarifeño-Saldivia E, Uribe E. 2024. Biodegradation of polystyrene by *Galleria mellonella*: Identification of potential enzymes involved in the degradative pathway. Intl J Mol Sci 25 (3): 1576. DOI: 10.3390/ijms25031576.

Wang J, Wang Y, Li X, Weng Y, Wang Y, Han X, Peng M, Zhou A, Zhao X. 2022. Different performances in polyethylene or polystyrene plastics long-term feeding and biodegradation by *Zophobas atratus* and *Tenebrio molitor* larvae, and core gut bacterial- and fungal-microbiome responses. J Environ Chem Eng 10 (6): 108957. DOI: 10.1016/j.jece.2022.108957.

Wang S, Yu H, Li W, Song E, Zhao Z, Xu J, Gao S, Wang D, Xie Z. 2024. Biodegradation of four polyolefin plastics in superworms (larvae of *Zophobas atratus*) and effects on the gut microbiome. J Hazard Mater 477: 135381. DOI: 10.1016/j.jhazmat.2024.135381.

Wright RJ, Bosch R, Langille MGI, Gibson MI, Christie-Oleza JA. 2021. A multi-OMIC characterisation of biodegradation and microbial community succession within the PET plastisphere. Microbiome 9 (1): 141. DOI: 10.1186/s40168-021-01054-5.

Wu C, Ma Y, Wang D, Shan Y, Song X, Hu H, Ren X, Ma X, Cui J, Ma Y. 2022. Integrated microbiology and metabolomics analysis reveal plastic mulch film residue affects soil microorganisms and their metabolic functions. J Hazard Mater 423 (Pt B): 127258. DOI: 10.1016/j.jhazmat.2021.127258.

Xu L, Li Z, Wang L, Xu Z, Zhang S, Zhang Q. 2024. Progress in polystyrene biodegradation by insect gut microbiota. World J Microbiol Biotechnol 40: 143. DOI: 10.1007/s11274-024-03932-0.

Yadav R, Rajput V, Dharne M. 2021. Functional metagenomic landscape of polluted river reveals potential genes involved in degradation of xenobiotic pollutants. Environ Res 192: 110332. DOI: 10.1016/j.envres.2020.110332.

Yang S-S, Brandon AM, Flanagan JCA et al. 2018. Biodegradation of polystyrene wastes in yellow mealworms (larvae of *Tenebrio molitor* Linnaeus): Factors affecting biodegradation rates and the ability of polystyrene-fed larvae to complete their life cycle. Chemosphere 191: 979-989. DOI: 10.1016/j.chemosphere.2017.10.117.

Yang Y, Yang J, Wu W-M, Zhao J, Song Y, Gao L, Yang R, Jiang L. 2015. Biodegradation and mineralization of polystyrene by plastic-eating mealworms: Part 1. Chemical and Physical characterization and isotopic tests. Environ Sci Technol 49 (20): 12080-12086. DOI: 10.1021/acs.est.5b02661.

Yun J-H, Roh SW, Whon TW, Jung M-J, Kim M-S, Park DS, Bae J-W. 2014. Insect gut bacterial diversity determined by environmental habitat, diet, developmental stage, and phylogeny of host. Appl Environ Microbiol 80 (17): 5254-5264. DOI: 10.1128/aem.01226-14

Zhang K, Ma X, Tang H, Li X, Mao C. 2024. Gut microbial comminoty in *Tenebrio molitor* larvae responsed to PS and PE within 6 hours. Intl Biodeterior Biodegrad 193: 105853. DOI: 10.1016/j.ibiod.2024.105853.

Zhang Y, Pedersen JN, Eser BE, Guo Z. 2022. Biodegradation of polyethylene and polystyrene: From microbial deterioration to enzyme discovery. Biotechnol Adv 60: 107991. DOI: 10.1016/j.biotechadv.2022.107991.